DC Microgrid Protection: A Comprehensive Review

Siavash Beheshtaein, Student Member, IEEE, Robert M. Cuzner, Senior Member, IEEE, Mojtaba Forouzesh, Student Member, IEEE, Mehdi Savaghebi, Senior Member, IEEE, and Josep M. Guerrero, Fellow, IEEE

***Abstract*— DC microgrids have attracted significant attention over the last decade in both academia and industry. DC microgrids have demonstrated superiority over AC microgrids with respect to reliability, efficiency, control simplicity, integration of renewable energy sources, and connection of dc loads. Despite these numerous advantages, designing and implementing an appropriate protection system for dc microgrids remains a significant challenge. The challenge stems from the rapid rise of dc fault current which must be extinguished in the absence of naturally occurring zero crossings, potentially leading to sustained arcs. In this paper, the challenges of DC microgrid protection are investigated from various aspects including, dc fault current characteristics, ground systems, fault detection methods, protective devices, and fault location methods. In each part, a comprehensive review has been carried out. Finally, future trends in the protection of DC microgrids are briefly discussed.**

***Index Terms*— DC circuit breaker, DC grounding systems, DC microgrid, fault analysis, fault location, power electronics, wide bandgap (WBG) semiconductors.**

I. Introduction

There are increasing examples of DC systems proving to be more efficient, less complex, have a high power transfer ratio and are lower cost than competing AC systems [1],[2]. At the point of use, DC systems make sense because many Distributed Energy Resource (DER) systems such as photovoltaic (PV), fuel cells and battery energy storage as well as the majority of loads such as Electric Vehicles (EVs) and light-emitting diode (LED) lights are natively DC powered.

Manuscript received September 04, 2017; revised October 04; accepted January 01, 2019. (Corresponding author: Siavash Beheshtaein.)

S. Beheshtaein and J. Guerrero are with the Department of Energy Technology, Aalborg University, Aalborg 9220, Denmark (e-mail: sib@et.aau.dk; joz@et.aau.dk)

R. Cuzner is with the Department of Electrical Engineering, University of Wisconsin-Milwaukee, Milwaukee, WI 53211 USA (e-mail: cuzner@uwm.edu)

M. Forouzesh is with the Department of Electrical and Computer Engineering, Queen's University, Kingston, ON K7L3N6, Canada (e-mail: m.forouzesh@queensu.ca)

M. Savaghebi is with the Electrical Engineering Section, The Mads Clausen Institute, University of Southern Denmark, Odense, Denmark (e-mail: mesa@mci.sdu.dk)

Color versions of one or more of the figures in this paper are available online at http://ieeexplore.ieee.org.

An additional advantage to DC systems is power quality impacts to public utility grids. Reactive power flow and frequency regulation are managed at lower cost and risk because of such systems, if there is any AC interface at all, will only connect through a single point of interface [1]. Examples of the growth and proliferation of DC include the use of multi-terminal High Voltage DC (HVDC) distribution systems to integrate renewables into electrical utility grids in Europe and China [3],[4] mobile transportation systems with integrated power and energy management applied to ships, aircraft and vehicles [5],[6] and electrification of remote areas through local DC microgrids that incorporate PV and battery energy storage into community and home electrical systems [7],[8]. DC microgrids are a convenient mechanism for integrating DERs and local loads into a fully integrative system with at least one point of interface to the AC electrical grid through a bi-directional AC to DC converter. All of the above examples may be referred to as either a DC microgrid in the classical sense (having a connection to the grid) or as an islanded DC microgrid (i.e., in the case of transportation systems). Despite numerous advantages, designing an appropriate protection system for DC microgrids remains a significant challenge over the past ten years. The challenge stems from the nature of dc fault current, which can rapidly increase to more than a hundred times of the nominal current during sudden fault inception and has no naturally occurring zero crossing point [9], [10] (which is a principal mechanism upon which AC electromechanical circuit breakers rely for arc extinction and eventually fault isolation). In order to address the challenges of DC microgrid protection, proper grounding architecture, fast and efficient fault detection strategy, fault current limiting method, and a proper DC circuit breaker are required.

Grounding in DC microgrids relates to various design goals and system considerations including grid reliability, minimization of leakage current during the normal condition, enabling ground fault detection, safety of equipment and personnel under faulty conditions. A proper grounding system has to be proposed with respect to safety, fault ride-through capability and ease of ground fault detection [11]. Considering the DC fault current characteristics, the fault must be identified and located in a timely, reliable way in order to prevent any damage to the equipment. Due to the fast rate of change of sudden inception of dc fault current, the coordination of the protective relays is also very difficult [10],[12]. Up to now, five main classes of fault detection methods including overcurrent,

This article has been accepted for publication in a future issue of this journal, but has not been fully edited. Content may change prior to final publication. Citation information: DOI 10.1109/JESTPE.2019.2904588, IEEE Journal of Emerging and Selected Topics in Power Electronics

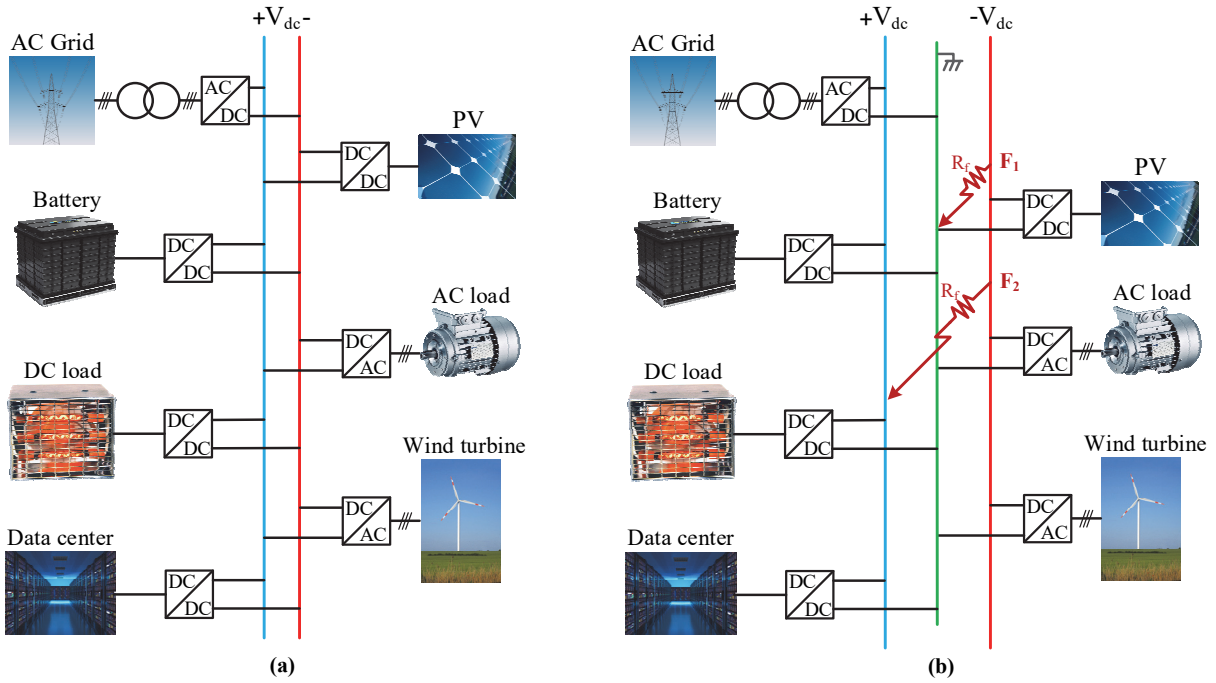

Fig. 1. DC Microgrid bus architectures. (a) Unipolar DC bus. (b) Bipolar DC bus with a voltage balancer.

directional overcurrent, current derivative, differential, and distance based strategies have been proposed. Fault location methods, including passive and active methods, in DC microgrids are an even much more demanding issue because the dc line resistance and reactance are considerably lower than in AC systems. Cost, computation burden, simplicity, and performance are competing requirement that such be evaluated when designing an appropriate fault detection/location strategy. Isolating the fault is accomplished by designing a proper DC circuit breaker (DCCB) to bring the DC microgrid back to a safe operational mode. This includes the complete air-gap, or galvanic isolation of the fault from the system. Concerning dc fault current characteristics, the DCCB must have the key features, including fast response, galvanic isolation, high reliability, low conduction loss, long lifetime, and low cost [9],[13]. According to the expected requirements, DCCBs must be selected from available devices or developed to meet the expectations.

In this paper, unless otherwise distinguished, fault refers to a short-circuit that is applied from any line to ground, across two lines or as two lines to ground faults occurring anywhere in the system. The sudden-inception short-circuit fault exhibits the most challenging fault behavior, and any feasible fault protection approach must be capable of addressing this scenario in order to mitigate equipment damage. This paper first provides a comprehensive analysis of the DC fault current in Section 2 to highlight the importance of fast fault detection, location, and isolation. Section 3 investigates different types of grounding systems for dc microgrid regarding stray current, common mode voltage, ease of fault detection and fault ride-through capability. Then, in Section 4, different types of fault detection methods including overcurrent, directional overcurrent, current derivative, differential, and distance are reviewed. The limitations, advantages, and applications of each protection method are discussed. Section 5 introduces and compares different protective devices including fuses, mechanical DCCB, solid-state DCCB, hybrid DCCB, and Z-source DCCB in terms of three main key features including cost, response time, and losses. Finally, Section 6 presents different types of fault location approaches including Traveling Wave (TW), differential, local measurement, and injection-based methods.

II. DC Fault Analysis

DC microgrids are categorized into different topological configurations, such as multi-terminal, zonal, and DC looped. The decision to choose a specific topology of DC microgrid depends on the application, reliability level, and voltage level [14]. For example, the U.S. navy focuses on developing zonal DC microgrid to achieve a shipboard system with high survivability, high power density, as well as low implementation cost [15]. Regardless of the different topological configurations of the DC microgrids, there are two types of DC bus architectures: unipolar DC bus topology using two-level Voltage Source Converters (VSCs) (see Fig. 1 (a)) and bipolar bus topology using three-level neutral-point-clamped VSCs (see Fig. 1 (b)). The bipolar DC bus topology has different advantages over unipolar, including more power capacity, increased reliability, and flexibility in the connections between loads and DGs [16].

One of the most straightforward topology to build the bipolar DC microgrid is using two-cascaded rectifier at DC side (see Fig. 2 (a)). In order to prevent DC voltage offset, which could

This article has been accepted for publication in a future issue of this journal, but has not been fully edited. Content may change prior to final publication. Citation information: DOI 10.1109/JESTPE.2019.2904588, IEEE Journal of Emerging and Selected Topics in Power Electronics

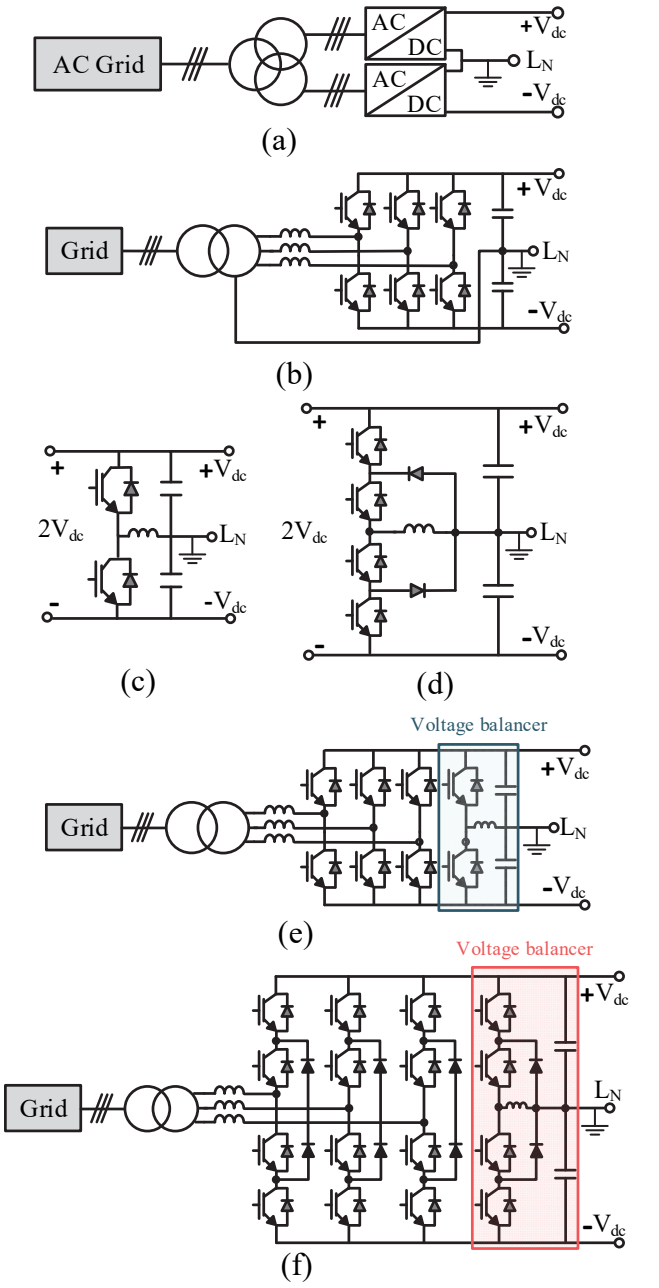

Fig. 2. (a) Bipolar DC system with two cascaded VSCs, , (b) Bipolar DC system with VSC that neutral line is connected to DC mid-point, (c) Buck/Boost-type voltage balancer, (d) Three-level Buck/Boost-type voltage balancer (e) Bipolar DC system with VSC with a DC voltage balancer, (f) Bipolar DC system with NPC converter with a DC voltage balancer.

happen due to the series connection, a transformer with double secondary windings is required. This may lead to a higher size and cost. To address this issue, other one-converter based topologies such as VSC with a neutral line connected to DC mid-point and NPC converter have been proposed (see Fig. 2(b)). In the VSC with a neutral line connected to DC mid-point, the DC component of the current may lead to transformer saturation [17]. On the other hand, the NPC converter has an inherent voltage-balancing problem, and there is no guarantee to balance the DC voltage during all the operating conditions [18]. In order to deal with the voltage balancing issue in these two configurations, a well-designed voltage balancer is needed to stabilize the DC bus voltage. A simple two-level and three level voltage balancers, which are used for VSC with a neutral line connected to DC mid-point and NPC converter, are respectively shown in Fig. 2 (c) and (d) [17]. These voltage balancers could integrate into three-phase rectifier (see Fig. 2(e)) and NPC converter (see Fig. 2(f)).

Regardless of the DC microgrid topology, the DC fault could occur either in the DC bus or in the DC cables that interconnect the microgrid components. Since simplicity of the microgrid is the goal of a DC microgrid, DC bus and DC interconnections are intended to act as a single point of energy interface between Distributed Generators (DGs), Energy Storage Systems (ESSs) and loads. From a protection standpoint, the down-side is that a fault on a DC bus or DC cable connection has the simultaneous effect on DGs, ESSs and loads which may all contribute to the fault current. Therefore, if the protection system design is inadequate, a single fault anywhere within the system can have unrecoverable impacts.

A. Battery and Load DC Fault Analysis

The battery may be far away from the DC bus; therefore, it has to be connected to the bus with cables. While the fault occurs in either DC bus or line, the fault current can be presented as follows [18]:

$$i_{batt}(t) = \frac{v_{batt}}{R_{batt} + R_{LB}}\left(1 - e^{-t/\tau_{batt}}\right) \quad (1)$$

$$\tau_{batt} = \frac{L_{batt} + L_{LB}}{R_{batt} + R_{LB}} \quad (2)$$

where R_{batt}, L_{batt}, R_{LB}, *and* L_{LB} are internal resistance and inductance, and line resistance and inductance, respectively.

On the other hand, the loads are categorized into constant impedance, constant power, and constant current. Based on the type of load, the fault current measured by load could be calculated.

B. VSC DC Fault Characteristics

The microgrid takes advantage of the VSC, which interfaces to the ac side through an inductor (L_{ac}) and to the DC side through a capacitor (C) as shown in Fig. 3 (a). Because of VSC structure, while the fault is exerted, first the DC side capacitor discharges through the DC network, then the fault current contribution from the converter interfaced sources forms the latter part of the response (See Fig. 3 (b)). Capacitor discharge will result in high current amplitude that could damage VSC components and other components in series with the fault. If fault current ride-through is a part of the protective strategy [19] then the excessive peak fault current must be taken into consideration as part of both system and component design processes.

On the other hand, if the same "breaker-based" protective paradigm of AC systems is applied to DC systems, where the protective devices mitigate faults, thereby eliminating the un-mitigated fault current characteristics from the connected component operational scenarios, then a fast protection device

This article has been accepted for publication in a future issue of this journal, but has not been fully edited. Content may change prior to final publication. Citation information: DOI 10.1109/JESTPE.2019.2904588, IEEE Journal of Emerging and Selected Topics in Power Electronics

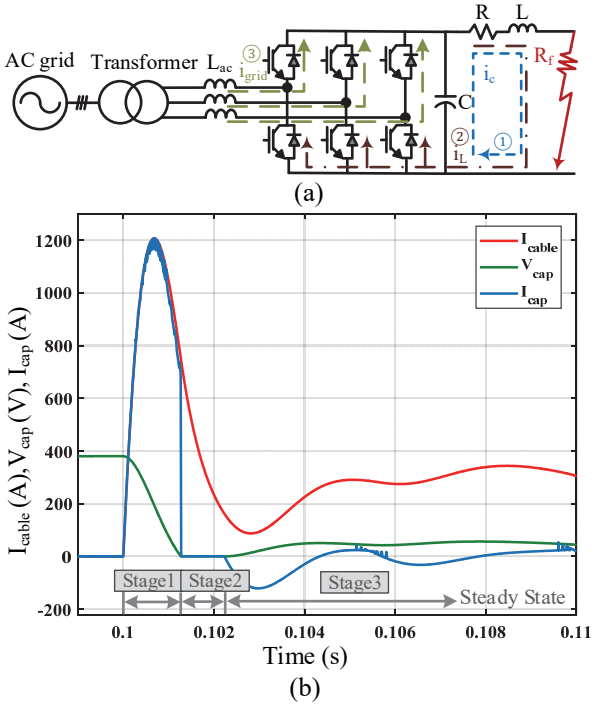

Fig. 3. (a) Equivalent scheme of VSC under a short-circuit fault, (b) Cable current i_{cable}, DC-link capacitor voltage V_{cap}, and capacitor current I_{cap} during the short-circuit fault.

is required to prevent damage. To understand and analyze the DC fault characteristics, the nonlinear system is solved by defining three different stages including capacitor discharge stage, diode free wheel stage, and grid-side current feeding stage. As shown in Fig. 3. (a), each stage current circulates in different loops. The overall DC fault current, regarding all of these stages, is presented in Fig. 3 (b).

1) Capacitor Discharge Stage (Natural response)

Once the fault occurs in the DC microgrid, the capacitor starts discharging through cable impedance as shown in Fig. 4 (a). In this stage, the peak value of fault current could go up to 100 times of the VSC rated current, depending on the internal resistance of the DC filter capacitor, capacitor value and cable inductance from the capacitor source to the fault location (see Fig.3. (b)). Fig. 4(a) shows the equivalent the RLC circuit. Its response in the Laplace domain can be written as [16]:

$$i(s)=\frac{V_C(0)/L+i_L(0)s}{s^2+\frac{R}{L}s+\frac{1}{LC}} \tag{3}$$

where $i_L(0)$ and $V_C(0)$ are initial the current through inductor and voltage across the capacitor, respectively. r and L are the resistance and inductance of the cable from the converter to the fault point. R_f is fault resistance and R is the sum of r and R_f. In the time domain, the fault current i (t) can be expressed as:

$$i(t)=\frac{V_C(0)}{L(s_2-s_1)}\left[e^{-s_1t}-e^{-s_2t}\right]+\frac{i_L(0)}{s_2-s_1}\left[-s_1e^{-s_1t}+s_2e^{-s_2t}\right] \tag{4}$$

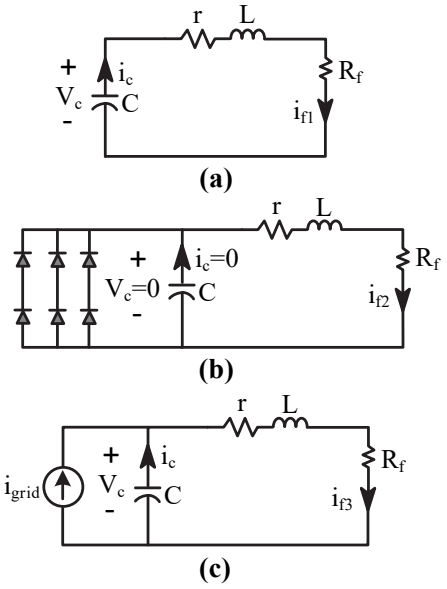

Fig. 4. Equivalent circuit for VSC under a short-circuit fault, (a) Stage1-capacitor discharge, (b) Stage2-freewheeling diodes, (c) Stage3- grid-side current feeding.

where s_1 and s_2 are the roots of the characteristic equation of (4), and are equal to,

$$s_{1,2}=-\alpha\pm\sqrt{\alpha^2-\omega_0^2} \tag{5}$$

In (5), α and ω_0 are respectively the damping factor and the resonance frequency defined as:

$$\alpha=\frac{R}{2L} \tag{6}$$

$$\omega_0=\frac{1}{\sqrt{LC_f}} \tag{7}$$

Based on the relationship between magnitudes of α^2 and ω_0^2, the form of the current response is determined, where for $\alpha^2>\omega_0^2$, $\alpha^2=\omega_0^2$, and $\alpha^2<\omega_0^2$ the fault current response would be over-, critically-, and under-damped, respectively. For example, the current response is obtained as follows for an under-damped system:

$$i(t)=\frac{V_C(0)}{L\omega_d}e^{-\alpha t}\sin(\omega_d t)+i_L(0)e^{-\alpha t}\left[\cos(\omega_d t)-\frac{\alpha}{\omega_d}\sin(\omega_d t)\right] \tag{8}$$

where $\omega_d=\sqrt{\omega_0^2-\alpha^2}$

2) Diode Freewheeling Stage (After V_C=0; Natural response)

If the source of AC power is lost at any point during the fault response process, then the capacitor will be discharging through the cable until its voltage reaches zero. In this case, the cable current commutates to the VSC freewheeling diodes (see Fig. 4 (b)). Thus, the cable current and current of each leg of the freewheeling diode are expressed as:

This article has been accepted for publication in a future issue of this journal, but has not been fully edited. Content may change prior to final publication. Citation information: DOI 10.1109/JESTPE.2019.2904588, IEEE Journal of Emerging and Selected Topics in Power Electronics

$$i_{cable} = I_0^{'} e^{-(R/L)t};\ i_{D1} = i_{cable}/3 \tag{9}$$

When capacitor voltage is zero the initial cable current ($I_0{}'$) may be almost ten times the nominal current value. Furthermore, the remaining inductive energy in the system may be significant while the dissipative loss in the system may be very low. As a result, if the time in this stage is very long, the freewheeling diodes are at high risk of damage. If the freewheeling stage is included as a part of fault mitigation, the time to fault isolation will be significant. Therefore, it is highly desirable to detect and isolate the fault during the first stage (capacitor discharge) before entering this stage.

3) Grid-Side Current Feeding Stage (Forced response)

In this mode, the VSC acts as an uncontrolled full-bridge rectifier and contributes to the fault current through the freewheeling diodes (see. Fig. 4 (c)) [20]. The fault current in this stage is calculated as:

$$i_{VSC} = i_{D1} + i_{D2} + i_{D3} = i_{ga,(>0)} + i_{gb,(>0)} + i_{gc,(>0)} \tag{10}$$

where $i_{ga,(>0)}$, $i_{gb,(>0)}$, and $i_{gc,(>0)}$ are respectively positive value of the phase-a, -b, and -c currents passing through the freewheeling diodes.

For phase a, the iga,(>0) is calculated as [20]:

$$\begin{aligned} i_{ga} &= I_g \sin(\omega_s t + \alpha - \varphi) + I_{gn} e^{-t/\tau} \\ \varphi &= \arctan\left[\frac{\omega_s (L_{ac} + L)}{R}\right] \\ \tau &= \frac{L_{ac} + L}{R} \\ I_{gn} &= \left[I_{g|0|} \sin(\alpha - \varphi_0) - I_g \sin(\alpha - \varphi)\right] \end{aligned} \tag{11}$$

where $I_{g|0|}$, φ_0, and L_{ac} denote the initial grid current amplitude and phase angle, and the grid-side inductance, respectively.

C. DC-DC Converters Fault Characteristics

As shown in Fig. 1, DC microgrids consist of power electronic point of source/load DC-DC converters that create an interface between DC sources and loads. Like VSC, these DC-DC converters are prone to failures caused by faults in the DC system. As shown in Fig. 3(b), the short-circuit fault current can increase to 15 times of the nominal steady-state current due to capacitor discharge through un-controlled paths when the fault occurs. For example, in the certain converter and converter connection topologies, the fault conditions can force the commutation of diodes to the on-state, forcing the fault current through where the fault current cannot be interrupted by any mechanism inherent to the converter topology [21], [22]. This phenomenon is detrimental to semiconductor switches due to the low short-circuit withstand of these components. Hence, fast fault detection and fault current interruption are required internal to the DC-DC converters to prevent failures due to short circuits [23], [24].

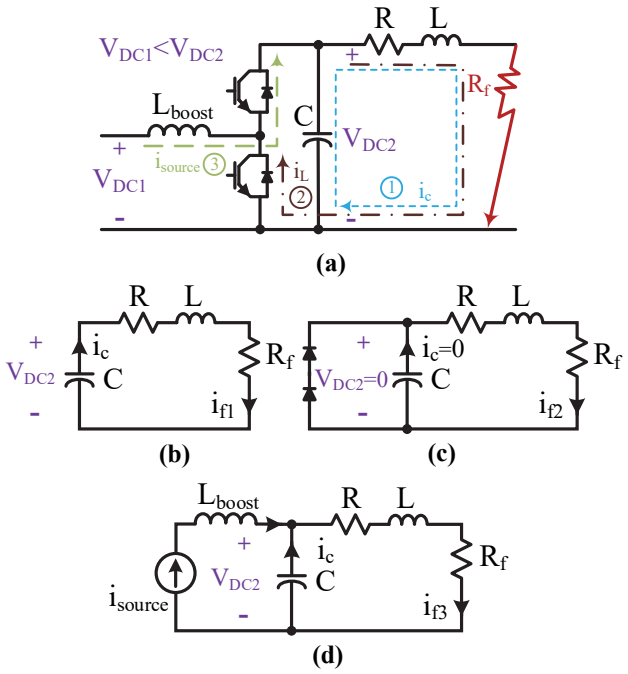

Fig. 5. (a) Boost DC-DC converter under short-circuit fault condition, (b) Stage 1 - capacitor discharge, (c) Stage 2 - freewheeling, (d) Stage 3 - input source side feeding.

If the constraints, such as cost, prohibit such an approach, then the external protective system must be designed mitigate any condition that may cause internal the inter-connected converters, i.e. through correctly placed fast acting fuses or DCCBs in all current conducting ports of the inter-connected converters.

Fig. 5 (a) illustrates the short-circuit fault condition in boost converter as an example of a traditional step-up non-isolated DC-DC converter. The nonlinear performance of fault current in boost converter is mainly like VSC with three stages including capacitor discharge stage (see Fig. 5 (b)), diode freewheeling stage (see Fig. 4 (c)), and input source feeding stage (see Fig. 5 (d)). If an instantaneous protective scheme has not been adopted for boost converter to quickly drive down the fault current from the input source within several microseconds, the short-circuit current will increase gradually until system breakdown [25]. If the mechanism for protection does not inherently provide galvanic isolation of the fault from the system, as is the case with the purely Solid State Circuit Breaker (SSCB) then an additional mechanically isolating device must be included in the switch mechanism. This can be a no-load set of isolating contacts (for both positive and negative feeds) that open up once the fault current has been driven to zero by the SSCB.

Fig. 6 (a) illustrates the short-circuit fault condition in buck converter as an example of the traditional step-down non-isolated DC-DC converter. The transient fault current is a little different in buck converter as the diode freewheeling current is restricted to the inductor current (see Fig. 6 (c)). This is because of inductor current (i_L) in buck converter cannot change instantaneously in the faulty conditions.

This article has been accepted for publication in a future issue of this journal, but has not been fully edited. Content may change prior to final publication. Citation information: DOI 10.1109/JESTPE.2019.2904588, IEEE Journal of Emerging and Selected Topics in Power Electronics

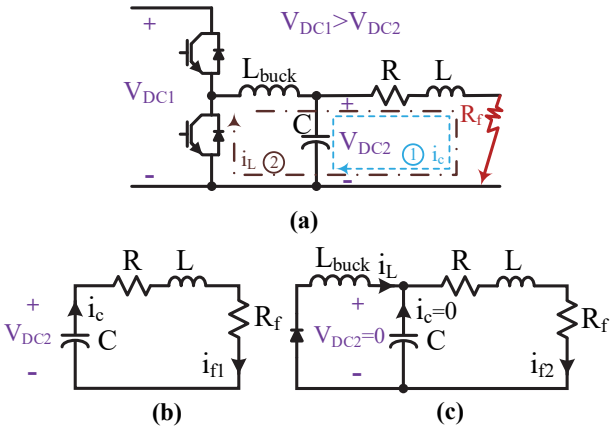

Fig. 6. (a) Buck DC-DC converter under short-circuit faulty condition, (b) Stage 1 - capacitor discharge, (c) Stage 2 – freewheeling.

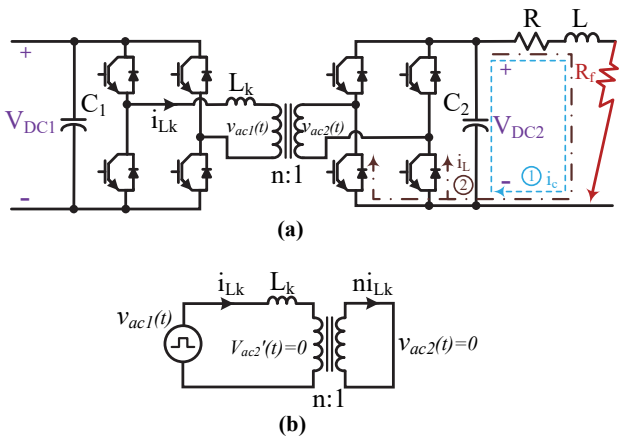

Fig. 7. (a) Isolated DAB DC-DC converter under secondary side short-circuit faulty condition, (b) Its equivalent AC circuit.

This behaviour makes buck converter intrinsically immune to short-circuit. One can design the inductor and output capacitor in a way to limit the short-circuit current to a specific required value [26]. Since the inductor in this circuit plays a dual role of both fault current limitation and pulse voltage attenuation during normal operation, the inductance can be relatively large. Therefore, approaches that depend upon buck converter current limiting must either accept long fault recovery times or include dissipative elements in the freewheeling path to drive down the fault current quickly when the fault occurs.

Fig. 7 (a) illustrates the short-circuit condition in a well-known and widely utilized buck-boost isolated DC-DC converter known as Dual Active Bridge (DAB) converter. Because of using transformer leakage inductance, the DAB converter can inherently isolate fault current from the source without any additional fast controller [27]. As a result, the DAB switching transistors will often switch at a very fast rate, which along with the low inductance, provides a fast and well-controlled current limiting capability during short-circuit fault conditions. The DAB also provides an inherent means of galvanic isolation due to input/output transformer isolation. Some researchers have investigated the exploitation of this feature for fault isolation [28]. The transient short-circuit fault in the DAB converter consists of a capacitor discharge stage and freewheeling stage. In the freewheeling stage, the natural transient response of uncontrolled bridge diodes rules until the converter reaches its steady-state value and the fault current in this stage (i_L) passes through two legs of the bridge freewheeling diodes [29]. In this mode of operation, the DAB operates as a Single Active Bridge (SAB) where the control mechanism shifts from the control of phase shift between actively commutating transistors on primary and secondary sides to active commutation of transistors only on the primary (source) side. Fig. 7 (b) demonstrates the AC equivalent circuit of the DAB converter when a short-circuit fault happens at the secondary side. This can be used to calculate the steady-state short-circuit current in DAB converter. The most general modulation method of the DAB converter named Triple Phase Shift (TPS) control [17] can be considered to modulate both converter bridges independently for power transfer control and fault current control. This control approach provides a more robust means of transition between normal and faulted modes when compared to DAB/SAB mode transitions. In TPS, an inner modulation Phase Shift (PS) angle M_1 is considered between primary bridge switches S_1 and S_4, an inner PS M_2 is considered between the secondary bridge switches Q_1 and Q_4, and an outer PS M_3 is considered between the corresponding switches in primary and secondary bridges (S_1 and Q_1). The converter RMS inductor current during the steady-state operation at maximum power transfer can be expressed in (12) (with maximum inner PS modulations M_1=180° and M_2=180°, and maximum outer PS modulation M_3=90°) [27].

$$i_{Lk\_RMS} = \frac{1}{4 f_s L_k}\sqrt{\frac{V_{dc1}^2 + n^2 V_{dc2}^2}{3}} \tag{12}$$

where f_s is the switching frequency, n is the transformer turns ratio, and V_{dc1} and V_{dc2} are DC voltages at the primary and secondary sides, respectively.

During secondary side fault (as shown in Fig. 7 (b)), the terminal voltage V_{dc2} and hence V_{br2} become zero, and by substituting this value in (12), the RMS value of fault current (i_{Lkf}) will be as (13).

$$i_{Lkf\_RMS} = \frac{1}{\sqrt{3}}\frac{V_{dc1}}{4 f_s L_k} \tag{13}$$

The magnitude ratio of the fault current over converter rated current can be obtained as

$$\frac{i_{Lkf\_RMS}}{i_{Lk\_RMS}} = \frac{V_{dc1}}{\sqrt{V_{dc1}^2 + n^2 V_{dc2}^2}} \tag{14}$$

Thus, (14) shows that the RMS fault current is always lower than the rated current when outer PS is M_3=90°. Moreover, when $n = V_{dc1}/V_{dc2}$ the RMS value of the fault current in DAB converter is only 0.707 times of its rated current. Similar calculation can be derived for the short-circuit fault at the primary side of DAB converter and the result is identical to the short-circuit current of the secondary side. To reduce the circulating current in DAB converter, it is desirable to operate it with M_3=45° outer PS and in this case the fault current would be i_{Lkf_RMS}=1.31i_{Lk_RMS} [29]. Therefore, it is curial to have a boundary when the converter fault current surpasses its

This article has been accepted for publication in a future issue of this journal, but has not been fully edited. Content may change prior to final publication. Citation information: DOI 10.1109/JESTPE.2019.2904588, IEEE Journal of Emerging and Selected Topics in Power Electronics

maximum current. This boundary can be selected as $2i_{Lk\_RMS}$, because most semiconductor switches can withstand twice their rated current in transients, which is within several milliseconds and limited to the junction temperature of semiconductor switches.

As mentioned above, the structure of some DC-DC converters can provide an inherent short-circuit fault immunity. For instance, similar short-circuit immunity feature of buck converter can be also observed in conventional buck-boost or multiple stage buck-boost converters that utilize an inductor at the output because inductor current cannot change instantly and hence short-circuit current will be restricted to the maximum inductor current [30]. Moreover, impedance source-based DC-DC converters can provide a buck-boost characteristic, and they are immune to open-circuit and short-circuit faults. When a moderate voltage gain is required, Z-source and quasi-Z-source DC-DC converters [31] can be used and when a high voltage conversion ratio is required Magnetically Coupled Impedance Source (MCIS) DC-DC converter can be employed [32]. The main drawback of these impedance source DC-DC converters is that the voltage stress on the switches is usually large in high step-up applications. This is detrimental to efficiency because using high voltage rating semiconductor switches with large R_{ds_ON} will cause high conduction losses.

Most isolated DC-DC converters have a buck characteristic and hence can limit the output current in case of short-circuit fault. When high power applications are considered in a microgrid system, modular multilevel converters (MMC) can be implemented with different submodules. If electrical isolation is not required, VSC is a good candidate due to its fault-tolerant capability and low component count and cost. On the other hand, most isolated DC-DC converters have a buck characteristic and hence they are able to limit the output current in case of short-circuit fault. Among them, full-bridge and DAB are suitable candidates as they can provide active limiting of current between cells in case of output short-circuit. Both full-bridge and DAB variations of the MMC can be distinguished from other current limiting converters because these converters maintain complete control of the submodule capacitor current during fault scenarios. Hence, the capacitor discharge is completely eliminated from the fault characteristic. There is no possibility of damage to any part of the system, either internal or external, during sudden short-circuit fault inception assuming all parts of the converter are functional.

Furthermore, it has been demonstrated that fault recovery time of this converter is minimal because there is no need to charge up discharged capacitors when the system returns to normal operation following galvanic isolation of the fault (i.e. through some other means such as no-load isolating switches in the path of the fault). The DAB submodule based MMC has the additional advantage of providing transformer galvanic isolation between the source and the fault. Since DAB converters can be controlled as a current source at both bridges, they can actively control the fault current at both input and output sides. Hence, in the MMC structure, DAB converter is a valuable option for current limiting and an effective choice for high power applications [30]. In conclusion, a compromise between different characteristics of DC-DC converters such as power density, efficiency, fault current limiting, redundancy, and the cost is a necessity to meet DC microgrid standards.

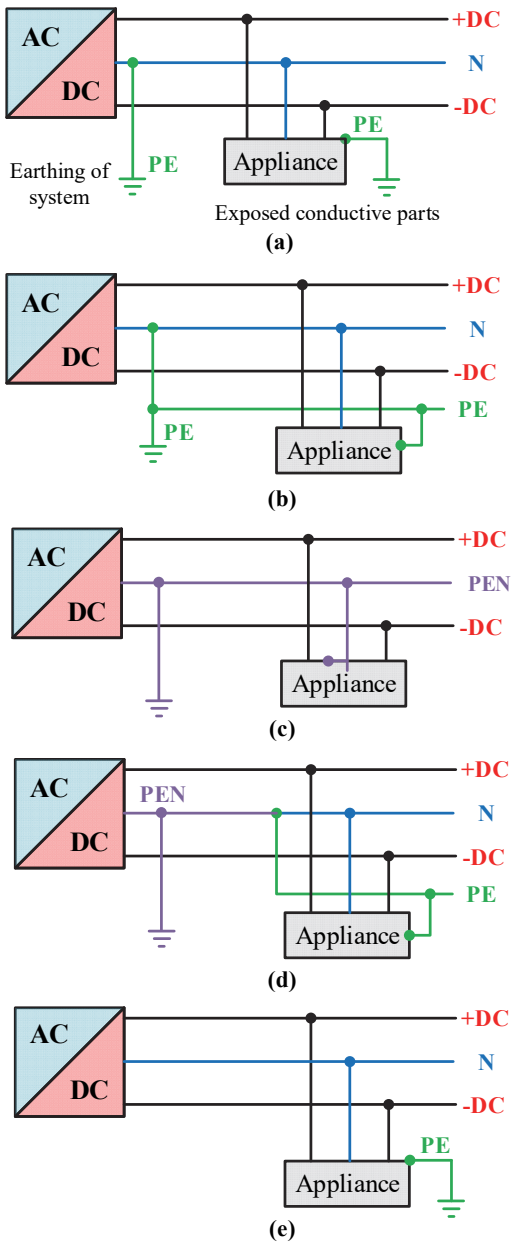

Fig. 8. DC microgrid grounding systems, (a) TT, (b) TN-S (c) TN-C, (d) TN-C-S, (e) IT.

III. Grounding Systems

Three main goals of the grounding system are to ease the detection of a fault, minimize DC stray current, and increase personnel/equipment safety by reducing Common-Mode Voltage (CMV) [33]. Stray current and CMV are related to each other by the grounding resistance. High grounding resistance results in very low stray current and high CMV. However, a low-resistance ground leads to low CMV and high stray current [14].

This article has been accepted for publication in a future issue of this journal, but has not been fully edited. Content may change prior to final publication. Citation information: DOI 10.1109/JESTPE.2019.2904588, IEEE Journal of Emerging and Selected Topics in Power Electronics

TABLE I. COMPARISON OF FOUR GROUNDING SYSTEMS.

	TT	TN-S	TN-C	IT
Safety of persons	• Good	• Good	• Good	• Good
Safety of property	• Good • Fault current less than a few dozen amperes	• Good • Poor • Fault current around a 1 kA	• Poor • Fault current around a 1 kA	• Very Good • Fault current less than a few dozen mA, but high for the second fault
Continuity of service	• Average	• Average	• Average	• Excellent
EMC	• Good • Risk of overvoltage/ voltage imbalance • Equipotential problems • Require to manage devices with high leakage currents	• Excellent • Less equipotential problems • Require to manage devices with high leakage currents • High fault current (transient disturbances)	• Poor • High fault current (transient disturbances)	• Poor (to be avoided) • Risk of overvoltage

According to IEC 60364-1, the DC grounding systems are categorized into five types including Terre-Terre (TT), Terre-Neutre (TN) [with three subclasses], and Isolated-Terre (IT) [15]. The first letter, including T and I, refers to the direct connection of the earth and no connection to the earth, respectively. The second letter including T and N denotes direct earthing of the exposed conductive parts and connection of the exposed parts to the earth neutral, respectively.

As shown in Fig. 8 (a), in the TT grounding system, neutral conductor of the converter and Protective Earth (PE) conductor of loads are separately connected to the ground point. The TT grounding system is straightforward to install, and the fault does not transfer to other parts of the grid; however, circulation of current and the possibility of high voltage stress are the main drawbacks of this grounding topology [34].

TN is the most commonly used DC grounding system. In this configuration, the converter middle point is connected directly to the ground and exposed conductive parts to the earthed neutral of the converter. Based on the TN grounding system, the connection of the conductive parts could be through a PE, neutral, or a combined PE and Neutral (PEN) conductor. The advantages of the TN grounding systems include having sufficient amount of fault current to be detected, requiring low grounding impedance, and the limiting fault current by adjusting the ground resistance; however, for high voltage applications, the touch voltage is high [35]. The TN topology has three subclasses including TN-S, TN-C, and TN-C-S. In TN-S, separate PE and N conductors are used (See Fig. 8 (b)); however, TN-C combines these two conductors to the PEN conductor to offer a cost-effective ground system (see Fig. 8 (c)). Thanks to the separation of the PE and N conductors, the TN-S system has the highest Electromagnetic Compatibility (EMC) among different types of TN grounding systems [36]. In addition, it has higher safety than TN-C, because, if the conductor gets disconnected, the protective features remain intact. As a result, this grounding system is suitable for information technology and communication networks. TN-C-S grounding topology is a combination of TN-C and TN-S to have maximum benefit from these two grounding systems (See Fig. 8 (d)). However, if the neutral conductor is disconnected and a fault occurs in the system, then the identification of the fault will be difficult. A viable solution is to ground neutral conductor at the source along with the route [37]. Such a grounding system is adapted in the United States, United Kingdom, Russia, Netherland, Switzerland, etc.

IT grounding system has no grounding point for the neutral point, and the appliance body is grounded separately (See Fig. 8 (e)). This configuration has advantages such as small line to ground (LG) fault current and ability to continue providing energy to the loads; however, its disadvantages include hard-to-locate fault and unpredictable fault current paths through the DGs when a second LG fault occurs [21]. Comparison of four main grounding systems can be summarized in Table I [36]. From the DC source-side grounding perspective, grounding modes in DC microgrid are typically divided into ungrounded (floating), grounded by solid ground, resistance, parallel resistors, diode, and thyristor. As shown in Fig. 9 (a), there is no connection between neutral and ground points. The main advantage of the ungrounded system is the continuous operation of DC microgrid during a single line to ground (SLG) fault conditions and minimal stray current [33]. In addition, as there is no need to connect any devices to neutral, this grounding system is simple and economical. However, the CMV level in the ungrounded system could be high and threaten personal safety. Moreover, due to the low ground current, fault detection is difficult. And, the second ground fault in another pole results in line-to-line (LL) fault possibly causing significant damage [22]. As a result, fault detection in the ungrounded or even the grounded system is a vital action toward improving the performance of these systems [21],[34]. Nevertheless, the ungrounded system is implemented in some application. For example, navy shipboard system is floating to guarantee continuity of energy supply to essential loads [38].

The solidly grounded system directly connects the neutral point to the ground. This system is depicted in Fig. 9 (b). The advantage of this system is limiting the CMV, increasing safety, decreasing the level of insulation. On the other hand, high fault current could melt lines, induce corrosion, and make a disturbance on telecommunication lines [33]. In the grounded system with a resistor (see Fig. 9 (c)), a resistor with certain value connects neutral to the ground. The main purposes of this grounding are limiting resonance overvoltage as well as limiting the transient short-circuit current within 2.5 times the proper value [39]. However, a higher value of resistance could slow the operation of Protective Devices (PDs). In grounding with parallel resistors, DC buses are connected to the ground by two parallel resistors of high resistance (see Fig. 9 (d)). This system takes advantages of the ungrounded system and

This article has been accepted for publication in a future issue of this journal, but has not been fully edited. Content may change prior to final publication. Citation information: DOI 10.1109/JESTPE.2019.2904588, IEEE Journal of Emerging and Selected Topics in Power Electronics

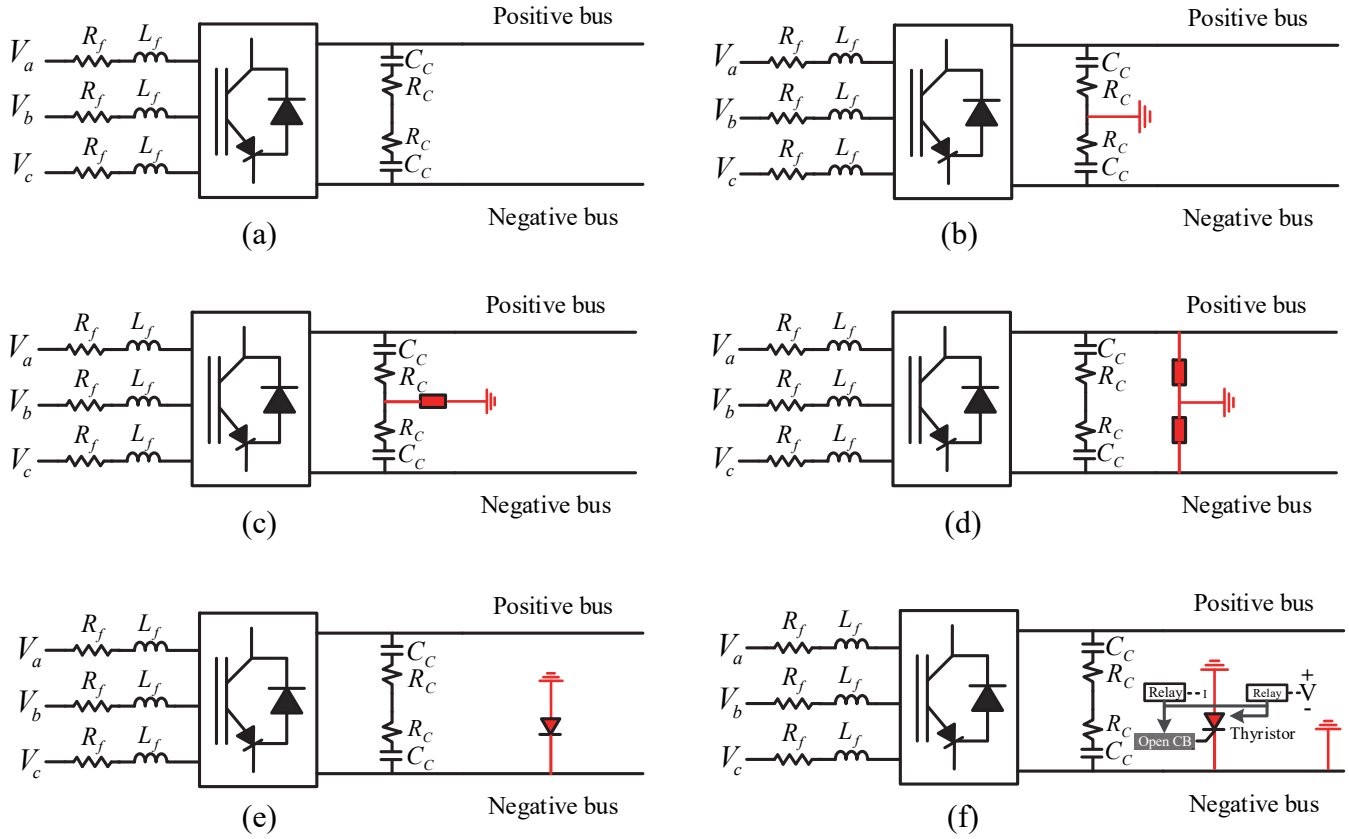

Fig. 9. DC microgrid grounding systems. (a) Ungrounded system, (b) Solidly grounded system, (c) Grounded system with a resistor, (d) Grounded system with resistors in parallel, (e) Diode grounded system, (f) Thyristor grounded system.

TABLE II. COMPARISON OF FOUR MAIN GROUNDING STRATEGIES.

Grounding system	Advantages	Disadvantages
Ungrounded system	• Continuous operation of DC microgrid during single line to ground fault • Low stray current • Simple and economical	• High CMV • Detection of the fault is difficult • Second ground fault in another pole results in line-to-line fault causes significant damage
Solidly grounded system	• Low CMV • Require a low level of insulation. • Fault detection is easy	• High fault current could melt lines, induce corrosion, and make a disturbance on telecommunication lines • High stray current
Diode Grounded system	• Low/moderate CMV	• High level of corrosion • Moderate/high stray current
Thyristor Grounded	• Low/moderate stray current	• Moderate/high CMV

grounded system with resistors, and remains in operation for a short time after the occurrence of the fault and fault location is based on the differential of resistors fault currents. However, this method has several disadvantages such as costly high-voltage, high resistances, generated heat in resistors causing an aging problem, and, hard to control overvoltage due to ungrounded neutral point [39].

Besides these grounding systems, recently, two power electronic-based grounding systems including diode and thyristor grounding have been proposed [33]. In diode grounding, as shown in Fig. 9 (e), the negative bus of DC microgrid is connected to the ground via a diode circuit. Once the level of voltage exceeds a definite threshold value, the negative bus will automatically be grounded. Due to this fact, the corrosion effect of DC currents is inevitable. In contrast to diode grounding, the thyristor grounded system controls the connection of negative part to the ground. This can be carried out by triggering thyristor gate when the negative-ground voltage exceeds a specific value. Furthermore, if a current sensor observes the decay of current, the gate-turn-off signal is sent to the thyristor to switch to ungrounded mode. The thyristor grounded system is shown in Fig. 9 (f).

Grounded and ungrounded systems have their disadvantages and advantages; thus a new grounding system is required to address the drawbacks of the conventional grounding systems. In [33], a reconfigurable grounding system was designed to operate based on the level of CMV. The system is ungrounded in normal condition to reduce stray-current-corrosion, and when CMC is high, the system switches to grounded mode to reduce CMV. Further investigation is required to standardize

This article has been accepted for publication in a future issue of this journal, but has not been fully edited. Content may change prior to final publication. Citation information: DOI 10.1109/JESTPE.2019.2904588, IEEE Journal of Emerging and Selected Topics in Power Electronics

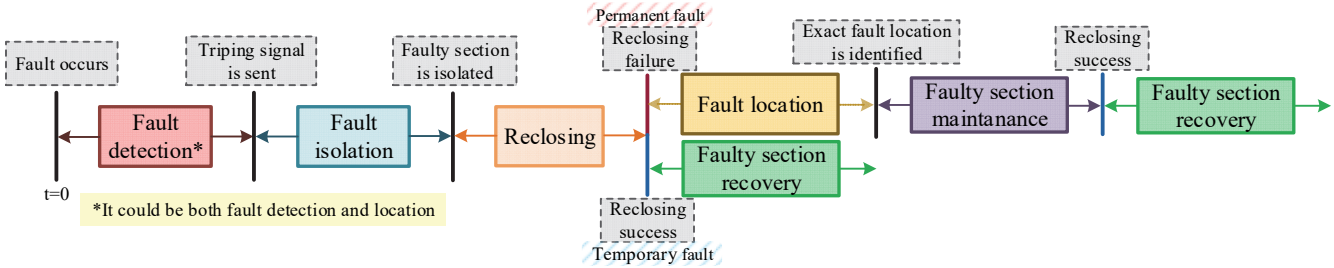

Fig. 10. DC fault protection process.

grounding systems for DC microgrids. The summary of four main grounding strategies is presented in and Table II.

IV. DC Fault Protection Process

As described in Section II, the fault current could increase to hundreds of the rated current. In such a condition, the main purpose of the protection system is first to identify (may also locate) the faulty section in the shortest possible time. Then, once it is identified, the tripping signal must be sent to the DC protective device to isolate the faulty section. These two stages must be performed very fast to prevent the power electronics devices from being damaged. The fault could be temporary or permanent. Due to this, if the fault is temporary, the protective devices must be reclosed after a certain amount of time to restore the isolated part. Otherwise, if the fault is permanent, the fault must be located to allow the repair crew to maintain that part. This DC fault protection process is shown in Fig. 10. It must be noted that different methods could be applied to find out the fault status and therefore avoid damaging the system due to reclosing failure.

V. DC Fault Detection Methods

In the DC microgrid, the line impedance is very low. As a result, fault current deviation is too high, and the fault current reaches hundreds of amp in less than a couple of milliseconds. As a result, the sensors have to have high sampling rates and speed, and the communication system must be very fast and reliable. Regarding implemented sensors, communication, and control systems, protection methods have to identify in a fast, reliable, and high precision manner.

Up to the present, several DC protection methods including overcurrent, current derivative, directional overcurrent, distance, and differential protections have been proposed to detect and identify the faulty section.

These DC protection schemes can be evaluated based on the following main features [23]:

- Speed: The protection method must identify the fault in a fast way to prevent the equipment from being damaged.
- Selectivity: The protection method must identify the faulty section. And for the external fault, the protection must not operate.
- Sensitivity: The protection method must detect all fault including high-impedance fault.
- Reliability: The protection system must isolate the faulty section when the primary protection or communication systems fail to operate.
- Cost.

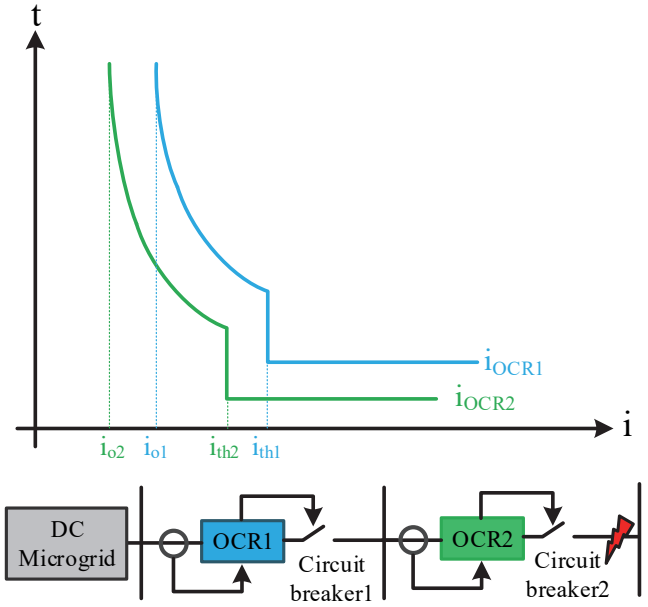

Fig. 11. Overcurrent protection coordination.

A. Overcurrent Protection

Similar to the traditional AC overcurrent protection, a threshold is considered to determine the occurrence of the fault.

In addition to fault detection, the implemented Overcurrent Relays (OCRs) have to be coordinated properly. As an example, time-current curves (TCCs), which composes of overload and instantaneous characteristics, of an upstream OCR and a downstream OCR installed in a dc microgrid is shown in Fig. 11. Once the measured currents by OCR1 or OCR2 are respectively above threshold I_{o1} and I_{o2}, the tripping signal the send to the associated CB after a specific time delay. It must be noted that the TCC of the downstream OCR must be below the TCC of the upstream OCR with an adequate margin to ensure selectivity. Furthermore, ultrafast turning-OFF speed of downstream PDs can reduce or even eliminate the mistrippings of upstream PDs.

The overcurrent protection is implemented for a dc microgrid where the rectifiers have an ability to limit the fault current [18], [40]. However, implementing such a protection method on more complex DC microgrid architectures may result in either longer fault clearance times or the disconnection of larger parts of a network than necessary in the event of a fault. In addition, for a compact dc microgrid, the time margin between upstream and downstream protection operation is small. In such a case, upstream OCR may act faster than the downstream OCR. One solution to address this low selectivity is to use a

TABLE III. COMPARISON OF FIVE MAIN DC PROTECTION METHODS.

	Overcurrent protection	Current derivative protection	Directional overcurrent protection	Distance protection	Differential protection
Speed	Moderate	High	Moderate	Slow	High
Selectivity	Moderate	Low	High	High	High*
Sensitivity	Low/Moderate	High	Low/Moderate	Low/Moderate**	High
Reliability	Low/Moderate	Low/Moderate	Moderate/High	Moderate/High	Low
Cost	Low	Low	Moderate	Moderate	High

* Highly depends on the existence of communication system. ** Among distance protection, active distance protection offers a medium or even high sensitivity.

communication link, which is based on the standard message of the IEC 61850 protocol, between the overcurrent relays to provide selectivity and disconnect only the faulty parts [41]. In [42], a framework is proposed based on the integration of unit-based protection, which has high sensitivity, speed, and selectivity, and overcurrent protection to have a fast and efficient operation and to minimize installation costs. Another disadvantage of overcurrent protection is its low sensitivity for high-impedance fault. In [43], a parallel LC filter is added to each pole to have resonance in specific frequency during the faulty conditions. Then, a Discrete WT (DWT) is utilized to extract this frequency for fault identification.

B. Current Derivative Protection

Once the fault happens, the current derivative increases from zero to a high value. This feature can be considered to identify a fault in a very short time. However, current derivative value depends on the cable length, line loading, and fault impedance. Due to this fact, it is very difficult to find a proper threshold and this threshold have to be adapted for each operating conditions. To deal with this issue first and second orders of the derivatives of the current are considered to detect the low and high fault impedance fault [44]. Furthermore, in order to measure the current derivative, sensors have to operate with high sampling rates. Using high sampling rates will amplify noise and may result in false tripping. To address this issue, an efficient filtering method is required to both have a little time delay and high nose cancelation capability.

C. Directional Overcurrent Protection

In a complex meshed DC microgrid, the direction of current could be from either side. Regarding this issue, implementing directional overcurrent protection could improve the selectivity. Recently, the directional overcurrent protection is proposed for a DC microgrid where a communication system exists [45],[46]. According to the proposed method, once the fault occurs, the magnitude and direction of fault current will be changed, then the direction of all branches is identified by aiding the communication system, this will help in locating the faulty line.

D. Distance Protection

Distance protection operates based on measuring the impedance from the point of measuring (POM) to the fault point. If the measured impedance is within a given distance value, a tripping signal will be sent to the associated CB after a specific time delay to achieve the protection selectivity. In order to have a fast distance protection system, there is no need to apply a time-consuming method to locate precisely the faulty point, and rough estimation of impedance will suffice for relay decision. In [20], voltage and current at the POM, and voltage at a closed point are measured; then, fault distance is estimated based on circuit analysis and perfuming an iterative calculation. Although this method uses an additional single iteration to improve the accuracy of distance, the estimated distance error increases when the fault resistance is high. Another approach is to measure resistance from a PD to the faulty point to offer several benefits such as low computation burden and requiring only cost-effective sensors and filter [47]. Since the line inductance has high value at high frequency, its value is negligible after several time constant. Due to this, the resistance is calculated after 10-20 ms, which is a quite long time. Another disadvantage of this method is having a low performance to locate fault for the case of short cable section and high-impedance faults. Measuring the line inductance based on the initial voltage across the VSC capacitor and Δi is another method for estimating fault distance [48]. However, the measured impedance is highly impacted by line loading and fault impedance. $\Delta^2 i$ is introduced besides Δi to address these issues [44]. Fast changing of the first and second order derivative of the line current requires implementing high sampling rates. In such a case, the high sensitivity of the fast measurement to noise makes this method less practical.

E. Differential Protection

Differential relay measures only the current amplitude of each side of a specific element by a current transducer and then, based upon the currents differential value, determines whether the fault has occurred or not. In [49], fault response of converter-interfaced DC systems is analyzed to investigate how transient system behavior, such as poor synchronization for the high change rate of a faulty condition, influences the operation of differential protection schemes. Then, this analysis quantifies the requirements for fast and accurate fault detection. Finally, a central processing device that takes advantage of the natural properties of DC differential current measurements is designed to achieve high-speed differential protection. In [50], comprehensive protection is presented for a Medium Voltage DC (MVDC) microgrid with various distributed energy sources including photovoltaic arrays, wind turbines, a fuel cell stack, an energy storage system, and mobile generators. The proposed protection schemes include communication-based differential protection with a solid-state switch for distribution lines, DC overcurrent protection as a backup for lines protection and communication-based DC directional overcurrent protection devices for both source and load protection to support bidirectional power flow. Nevertheless, similar to AC microgrids, differential protection has disadvantages such as the need for a communication system, being a high-cost

This article has been accepted for publication in a future issue of this journal, but has not been fully edited. Content may change prior to final publication. Citation information: DOI 10.1109/JESTPE.2019.2904588, IEEE Journal of Emerging and Selected Topics in Power Electronics

solution, no capability for backup protection, and being susceptible to current transducer errors.

All of these protection methods are compared in Table III, in terms of speed, selectivity, sensitivity, reliability, and cost.

VI. DC Protective Devices

PDs used in the DC system are broadly divided into AC circuit breakers (ACCBs) and DCCBs. ACCB is a simple and economical solution for the VSC-based High Voltage Direct Current (HVDC) system; however, it is not fast enough to prevent damage to the VSC's freewheeling diodes. In addition, employing ACCB leads to disconnection of the whole network. Another solution is a combination of ACCB and fast DC switches [51]; however, the slow time response of ACCB may damage the power electronic devices in a very short time. On the other hand, the increase in penetration of DG and energy demand results in a rise in fault current levels that may exceed the rating of the existing circuit breakers and loss of coordination of the overcurrent protection [52]. Replacing the network's facilities such as transformers, transmission and distribution lines, and circuit breakers with higher rating ones is a solution that is not cost-effective.

A. Breaker Based Architecture

The fuse, which consists of a link and a heat-absorbing material inside a ceramic cartridge, is used as a simplest and primitive protective device in the protection of DC systems for voltage up to 4200 volts. Fuses are ideal to apply in the DC systems with a low inductance (or high deviation of current) because the time for the fuse to reach melting point would be minimum [53]. Although the fuse is a low-cost protective device with a simple structure, it has disadvantages such low time response, requiring it to be replaced after a successful operation, and inability to discriminate between transient and permanent faults. As a result, CB technologies have been introduced to provide an appropriate alternative for the fuses. In the past years, different DCCBs technologies including Mechanical CBs (MCBs), SSCBs, Hybrid CBs (HCBs), and ZSCBs have been presented for DC systems.

For LV system fuses, Molded Case CBs (MCCBs) and MCBs are three conventional PDs [54]. However, these solutions have drawbacks such as slow time response and the need for maintenance or replacement. On the other hand, in LV systems, power converters limit the fault current to 2-3 times of the nominal load current and quickly shut down to have self-protection when the fault current exceeds the limit. As a result, the use of these PDs results in tripping of the source converter and creates a local blackout. Utilizing SSCBs is an alternative to overcome these limitations in the LV system. Although SSCB has a fast response in ranges of tens of microseconds, its relatively high conduction loss is the main drawback. Using Wide Band-Gap (WBG) semiconductor in SSCB is a solution to reduce the power losses [55],[56]. In addition, the voltage rating of the SSCB needs to be chosen significantly higher than DC bus voltage [57] and higher conduction loss in SSCBs requires bulky cooling systems. These drawbacks make SSCBs less attractive for HVDC applications. HCB is an appropriate candidate for HVDC systems because it has a relatively fast time response (few ms), low power loss, and a relatively low weight/volume [58].

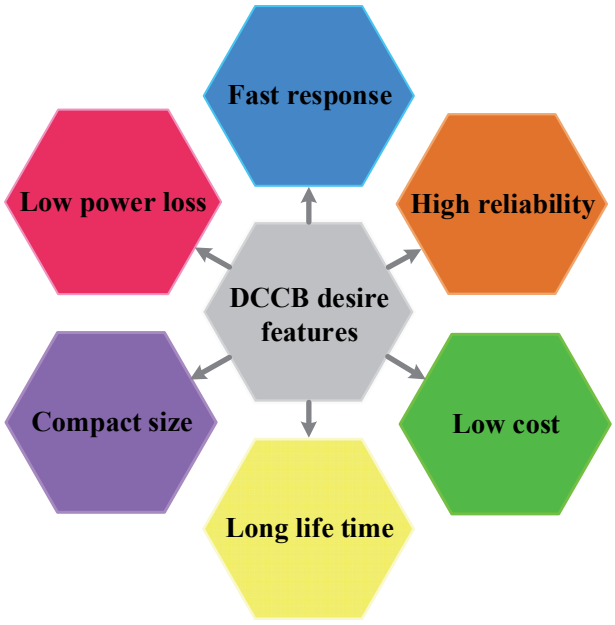

Fig. 12. Six desired key features of a DCCB.

Although HCB possesses many advantages, some challenges arise due to different reaction times and current rating of the MCB and the SSCB, dependence of mechanical contacts separation on the fault magnitude, need for an arc with a voltage higher than solid-state voltage drop and extinction of the MCB arc. In addition, high loop inductance leads to high commutation time and therefore high current fault, as well as high conduction time of the solid-state device is needed due to high commutation time [59]. Therefore, all aforementioned challenges must be considered for designing the HCB for a specific application. In shipboard MVDC integrated power systems, PDs must have a small size, low weight, high speed, and providing the 2-3kA continuous current rating [60]. As HCBs are heavy, too bulky, and too slow to interrupt the sudden inception of low-impedance faults and avoid tripping of converters in the unfaulty parts of the system, recent researches have been focused on enhancing WBG SSCBs technologies for the future shipboard MVDC microgrids [61],[62]. However, WBG SSCBs have some limitations such as achieving a required continuous current rating and controlling the amount of inductance to limit the current's rate of rising (*di/dt*). To achieve the required continuous current rating, one solution is paralleling multiple 1.0 cm^2 SiC Super Gate Turn-off Thyristors (SGTOs) that can operate for pulse switching at higher voltage and power ratings (e.g. 10 kV and 100 kA in the case of 16 parallel SGTOs) [63]. The DC system is required to detect and isolate faults in less than 5 ms or less, followed by a rapid configuration of the system to provide survivability [64],[65]. Since the nature of the DC system is different from the AC system, DCCB has to be designed differently to achieve six desired features as represented in Fig. 12.

1) Mechanical Circuit Breaker

Generally, operating mechanism of MCB are categorized into pneumatic, hydraulic, spring, and magnetic. Spring and

This article has been accepted for publication in a future issue of this journal, but has not been fully edited. Content may change prior to final publication. Citation information: DOI 10.1109/JESTPE.2019.2904588, IEEE Journal of Emerging and Selected Topics in Power Electronics

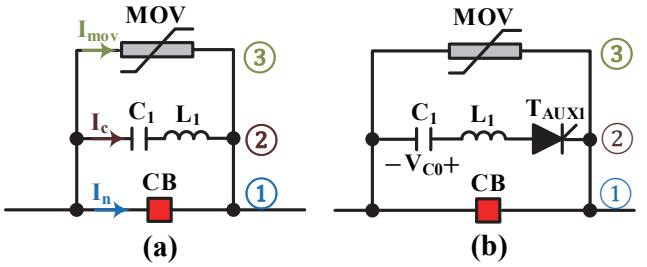

Fig. 13. MCB with (a) a passive commutation circuit, (b) an active commutation circuit.

magnetic operating mechanisms are more common in vacuum CBs, however the later one is more attractive because it has less moving parts and higher reliability. Recently, an operating mechanism based on repulsion coil, so-called Thomson coil, have gained more attraction because it has a simple structure and reduces MCB operation time to 1-3 ms [67],[68].

While the fault happens, the mechanical switch contacts are separated and electric arcs are created between the contacts. Due to the existence of the natural zero-crossing in AC microgrid, these mechanical switches is quite applicable, however, with the absence of the zero-crossing in DC microgrids, utilizing the mechanical switches will be restricted for several applications. Passive and active resonance circuits have been proposed to deal with this problem [66]. Regardless of the type of resonance circuit, the MCB is composed of three main parts including a mechanical switch, a commutation circuit, and an energy absorber circuit (see Fig. 13). The scheme of MCB using passive and active resonance circuits are shown in Fig. 13 (a) and (b), respectively.

In the passive resonance circuit, a capacitor and an inductor are connected in series, and the capacitor has not been pre-charged. During normal conditions, the mechanical switch conducts the load current with a low amount of loss, because the resistance is around ten μΩ for a well-designed mechanical switch [57]. Once the fault occurs, the mechanical switch opens and an arc is established. The arcing voltage initiates commutating of current from the load current path to the commutation path. Then the commutation circuit that has the capacitor and inductor in series generates a growing current oscillation. While the amplitude of oscillating commutation current (I_c) is sufficiently large, zero-crossing points are produced in the mechanical switch current (I_n) and mechanical switch completely interrupts current in its path at the first zero currents. During these two stages, the voltage of the mechanical switch is gradually increasing until it reaches a specific value. When the voltage exceeds a definite value, the current changes its path to an energy absorber circuit, which is typically a Metal Oxide Varistors (MOV) to absorb and dissipate the stored energy after an interruption. In this stage, the fault current decreases gradually to approach zero.

On the other hand, as shown in Fig. 13 (b), the active commutation circuit is made of a precharged capacitor, an inductance, and a thyristor switch/triggering gap. In this type of the MCB, when the interrupter is opened, the charged capacitor injects a negative current equal to fault current to make zero-crossing current instantly. The main advantages of MCBs are low power loss and relatively low cost; however, slow response time and limited current interruption capability are the main disadvantages.

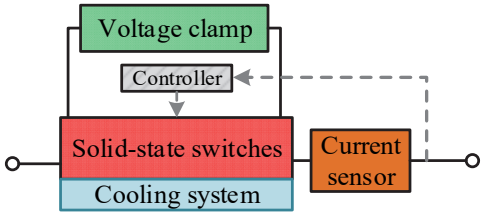

Fig. 14. A typical SSCB.

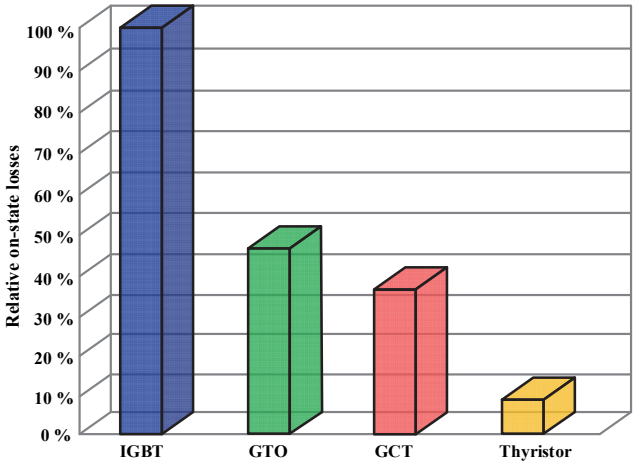

Fig. 15. Relative on-state losses.

2) Solid-state Circuit Breaker

Semiconductor-based switches could be used for DC circuit breaker to address the problem of slow time response. A typical SSCB is shown in Fig. 14, where a cooling system is used besides the semiconductor device to ensure high efficiency of the SSCB during the conducting condition.

Since the invention of the bipolar junction transistor, many Silicon (Si)-based semiconductor switching devices including Gate-off Thyristor (GTO), Integrated Gate-Commutated Thyristor (IGCT), Silicon Insulated-gate Bipolar Transistor (IGBT), and Metal-Oxide-Semiconductor Field-Effect Transistor (MOSFET) have been utilized for power electronics application [67]. Among the SS devices, thyristors have the lowest conduction losses. Such a low on-state loss of thyristor switch results in reduction of overall life-cycle costs of the SSCB and decreased investment on the cooling system of thyristor-based SSCBs. However, the main drawback of thyristors is not being able to actively turn off the current. This long switching response leads to high fault current. GTO, IGCT, and IGBT have the forced commutation capability, and they can be switched between 50 Hz to 20 kHz. It is reported that GTOs and IGCTs have much lower on-state losses than IGBTs [68]. Fig. 15. Shows the relative on-state losses of the thyristor, GTO, GCT, and IGBT [69],[70]. These solid-state devices can be commercialized for the maximum voltage rating of 6.5 kV[70]. For the medium voltage range, the silicon (Si) power MOSFET has high conduction losses and therefore it is not an appropriate option. Superjunction MOSFETs present a low specific on-state resistance in a range of 15-20 mΩ/cm^2 for voltage range under 600 V [57].

This article has been accepted for publication in a future issue of this journal, but has not been fully edited. Content may change prior to final publication. Citation information: DOI 10.1109/JESTPE.2019.2904588, IEEE Journal of Emerging and Selected Topics in Power Electronics

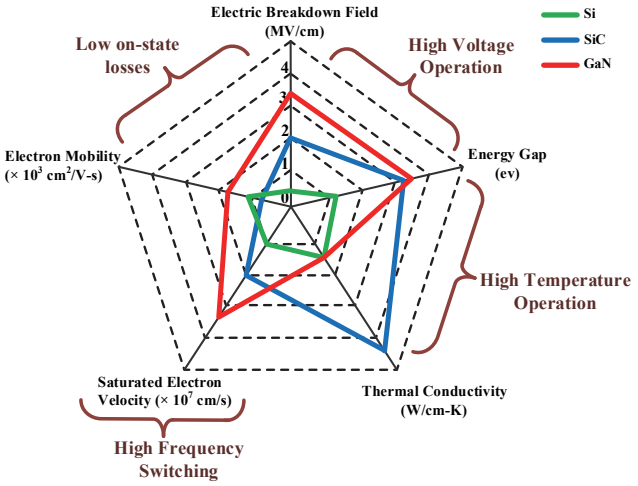

Fig. 16. Summary of Si, SiC, and GaN relevant material properties.

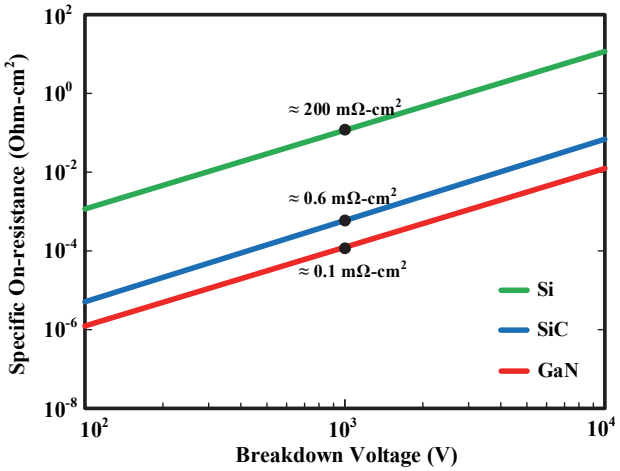

Fig. 17. Comparison of on-resistance of-of Si, SiC, and GaN.

During the last 50 years, Si power semiconductor devices have encountered many limitations such as blocking voltage capability, operation temperature, conduction loss, and switching frequency [71]. These limitations require the power devices to have a cooling system, as well as a bigger filter and passive components. WBG materials could address these limitations by offering outstanding characteristics such as low conduction loss, high-temperature capability, high voltage capability, and high-frequency capability. SiC-based devices and Gallium-Nitride (GaN)-based devices are two best candidates that could offer a good trade-off between theoretical characteristics and availability of material. The key characteristics of Si, SiC, and GaN materials are shown in Fig. 16 [72]. According to the third figure, GaN material presents low ON-state loss, better high frequency, and high voltage capability, however, compared to SiC, its thermal conductivity is lower.

Thermal conductivity allows better heat transmission from the device to the ambient. Therefore, the higher values of this property make the device suitable for the high-temperature application. As can be seen from Fig. 16, SiC and GaN can operate at much higher temperature. It is reported that SiC and GaN semiconductors could work in 600°C [73],[74] and 450°C [75], respectively. This characteristic of SiC devices makes them suitable candidates for aerospace and space missions [76]. The voltage rating of a device depends on breakdown voltage, which is relied on the critical breakdown field (E_c). It is proved that E_c is proportional to the energy gap [77]. Regarding this fact, a higher value of E_c will allow the device to be more applicable for high voltage operation [78]. The higher E_c will also allow thinner drift layer with a higher doping concentration at the same blocking voltage, which leads to lower specific ON-resistance. Specific ON-resistance, which is independent of the chip size, can be presented in term of breaking voltage [79]:

$$R_{ON-sp} = \frac{3.351\times10^{-3} V_B^2 E_G^{-6}}{\mu_e \varepsilon_r}; \text{ for Si and SiC} \quad (15)$$

$$R_{ON-sp} = \frac{8.725\times10^{-3} V_B^2 E_G^{-7.5}}{\mu_e \varepsilon_r}; \text{ for GaN} \quad (16)$$

where μ_e, μ_r, V_B, and E_G are electron mobility, relative permittivity, breakdown voltage, and energy bandgap.

According to (15) and (16), R_{ON-sp} of Si, SiC, and GaN are plotted in Fig. 17. As it can be seen from this figure, for example for V_B=1 kV, the specific resistance of Si, SiC, and GaN are 200, 0.6, and 0.1 mΩ-cm^2, respectively. It means that in comparison with Si power device, the SiC power device has a remarkable low power loss.

With a higher saturated electron velocity, the minority carriers will be more quickly swept out of the depletion region during the turn-off transient, which results in enabling higher switching frequency. Increasing the switching frequency has two key benefits including size and weight reduction of passive components, which leads to a more compact device and better dynamic response of power device. However, the maximum switching frequency is limited by the device's switching loss. In unipolar devices such as MOSFET and Junction Field-Effect Transistor (JFET), switching frequency only depends on the charging and discharging of the parasitic capacitance. However, switching frequency of the bipolar devices such as Bipolar Junction Transistor (BJT) and IGBT relies on building and depletion of the stored excess carriers. This would lead to higher frequency capability of unipolar devices (see Fig. 18). For example, as shown in Fig. 18, the switching frequency of the MOSFET is roughly higher than the IGBT/Thyristor).

From the application point of view, in each range of frequencies and rating powers, a set of converters with a specific material are a suitable option. Thyristor switching devices are known as the best candidate HVDC. These devices work at the line frequency (50 or 60 Hz) because they have no gate controlled capability. IGCT, GTO, and Emitter Turn-Off (ETO) thyristors, which are the next generations of the original thyristor, have the force commutation capability and could have switching frequency between 50 to a few hundred hertz [80]-[81]. Since the blocking voltage of the Si-based thyristors is typically below that 6.5 kV, a series connection of them is required for very high voltage applications. Sic-Based thyristor is a promising solution to address this issue [80]. For the medium power applications such as WTs and PVs, IGBT devices are widely utilized for 600 to 6.5 kV and 10-20 kHz. However, as the voltage gets higher other solutions such as the

This article has been accepted for publication in a future issue of this journal, but has not been fully edited. Content may change prior to final publication. Citation information: DOI 10.1109/JESTPE.2019.2904588, IEEE Journal of Emerging and Selected Topics in Power Electronics

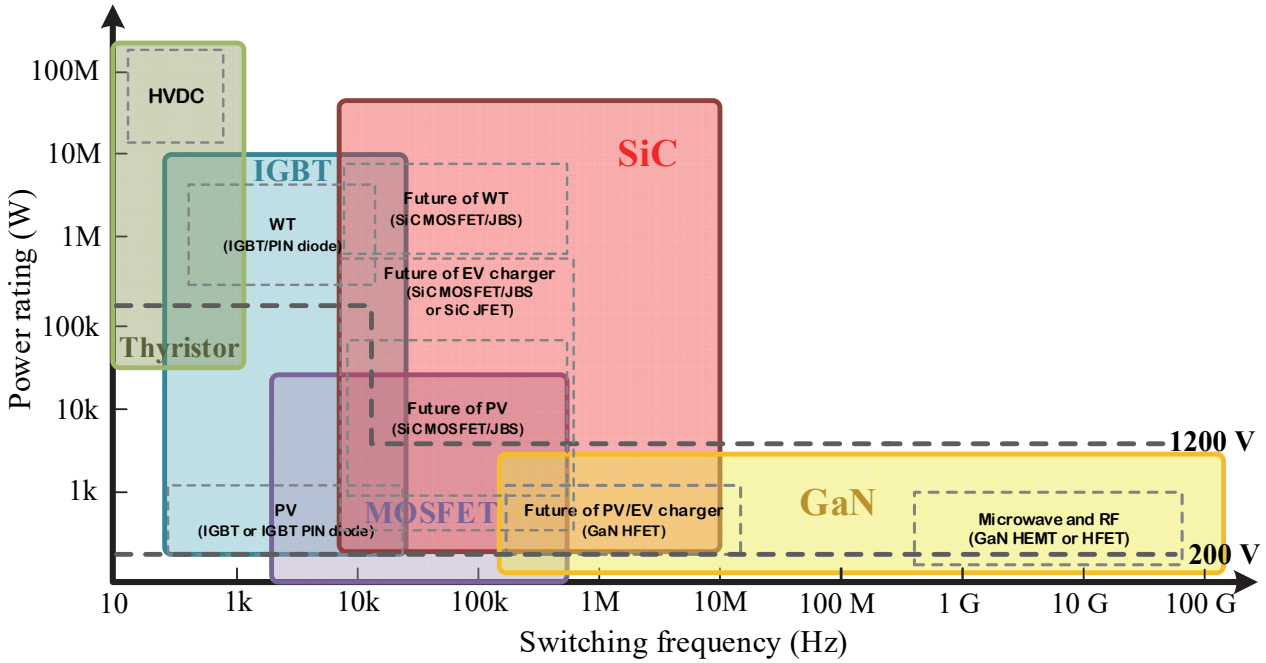

Fig. 18. Si, SiC, and GaN-based applications.

series connection of IGBTs and using SiC-IGBT must be considered. Cascaded IGBTs have different disadvantages including a need for snubber circuits for voltage balancing, being very bulky, low efficiency, and higher control complexity [82].

On the other hand, in order to address these issues, growing attention has been paid to replace Si IGBTs with high voltage SiC IGBTs (>10 kV) [83]. Thanks to no existence of the bipolar charge-storage mechanisms, the unipolar devices such as MOSFET and JFET could operate in higher switching frequencies. Having higher switching frequency capability, the unipolar devices could be built with a smaller cooling system and passive devices, leading to power devices with high power density [84]. However, with the increase of the blocking voltage, the on-resistance of MOSFET keeps growing and results in high power loss. Because of that issue, Si IGBT is more common than Si MOSFET for high voltage and current applications. Similar to bipolar devices, SiC unipolar power devices have much higher blocking voltages and switching frequency capability than Si one [71]. Compared to SiC MOSFET, SiC JFET has lower on-resistance higher operation capability and no concern about the oxide layer. These features make SiC JFET as an appropriate candidate for tough operating conditions such as SSCB and electric vehicle [85],[86]. However, "normally on" characteristics of SiC JFET prevents it from being widely used in industrial applications [87]. GaN power devices technology is categorized into vertical and lateral structures. Vertical GaN power devices have a similar structure to the Si/SiC counterparts. This type of GaN devices has superior advantages including very low power loss as well as small size. However, lower thermal conductivity as well as lack of good-quality bulk substrates, and inexpensive GaN wafers prevent this type of GaN power devices from being commercialized. On the other hand, lateral Heterojunction Field-Effect Transistors (HFETs), which is also known as High Electron Mobility Transistors (HEMTs) are commercialized and available at relatively maximum rates of 650 V and 100 A. The HFET GaN power device has advantages such as very low R_{ON} per squared breaking voltage, very low power loss and very high switching speed (up to 454 GHz) [88],[89]. These properties make these devices attractive for microwave, radio frequency (RF), and power electronic applications [90],[91].

As a conclusion, the employment of WBG materials in SSCB increases breakdown voltage capability and decreases ON-resistance. Higher breakdown capability and lower ON-resistance of the WBG materials avoids or significantly reduces the number of series-connected devices and parallel connection of Si device, respectively [92]-[93]. In addition, since energy burst during the faulty condition pushes the junction temperature above the silicon limit, ability to stand higher junction temperature under both static and dynamic conditions makes them be a proper candidate for SSCB applications [13]. Finally, the advantages of higher switching frequency capability of the WBG devices are a reduction of size and weight of passive components, which is a key factor for high-density power electronics [78]. As a result, employing WBG materials in SSCB will be a CB with higher efficiency and lower size. Although utilization of WBG materials in SSCBs has an outstanding outcome, several challenges have to be addressed to pay the way of widespread applications of WBG based SSCBs. These challenges include designing advanced gate-drive with active *dv/dt* and *di/dt* control, designing efficient Electromagnetic Interference (EMI) filter, and design better device packaging due to high temperature and fast switching,[75],[77],[83],[94],[95].

3) Hybrid Circuit Breaker

Each of the MCB and SSCB has its own drawbacks and benefits. HCB is a new class of CBs that combines both the MCB and the SSCB to take advantages of both [59]. As a result,

This article has been accepted for publication in a future issue of this journal, but has not been fully edited. Content may change prior to final publication. Citation information: DOI 10.1109/JESTPE.2019.2904588, IEEE Journal of Emerging and Selected Topics in Power Electronics

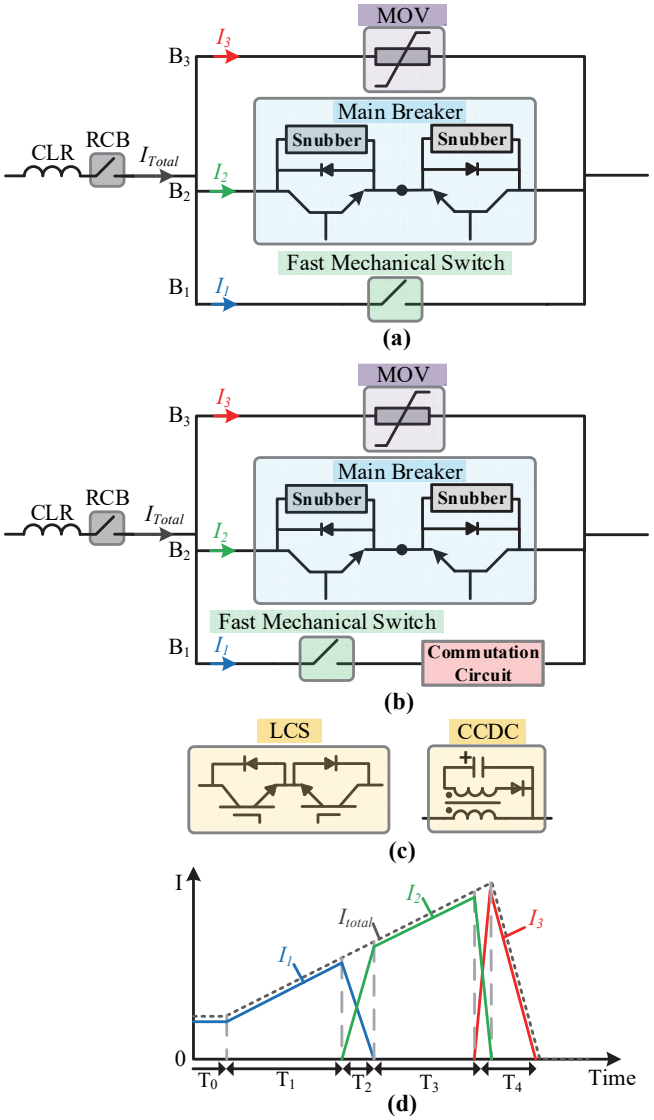

Fig. 19. HCB. (a) Structure of the conventional HCB, (b) Structure of the HCB with a commutation circuit (b) Commutation circuits, (c) Current waveform during the normal and faulty condition.

HCBs have advantages such as fast response, low power loss, and no arcing at the mechanical contacts.

As shown in Fig. 19 (a), a conventional HCB has three main parts including a mechanical switch (MS), a high-voltage SS switch as the main breaker (MB), and a MOV [96]. In addition, a Current Limiting Reactor (CLR) in series a Residual Circuit Breaker (RCB) may be added in series with these branches to limit the current rate of change and to isolate the faulty line completely. During the normal condition, the current passes through MS. When the fault is identified, the MS starts the opening of its contacts and sends turn-on signal to the MB. The established arc voltage is increased until it exceeds the voltage drop of MB. In this case, the current can be naturally commutated from the MS to the MB. The MB continues conducting current until the MS is able to block full voltage. At this point, the MB is turned off and the voltage increases quickly because of circuit inductors. While the voltage reaches breakdown voltage, the fault current commutes to the MOV to clamp voltage and approach the current to zero. Finally, when the fault current is zero the RCB is opened to isolate the faulty line from the DC grid to protect MOV from thermal overload [58].

In low voltage systems, the arc voltage of the MS is usually higher than the voltage drop of the MB; therefore, current commutation will happen naturally and there is no need for a commutation circuit. However, for the high voltage applications, the voltage drop of the MB increases up to the hundreds of volts and the arc voltage of the MS could not increase that high within a couple of milliseconds. As a result, a commutation circuit, such as Load Commutation Switch (LCS) and Current Commutation Drive Circuit (CCDC) (see Fig. 19 (c)), is necessary to ensure successful current commutation from MS to MB branches [70],[97].

Current waveforms of the HCB with the commutation switch (see Fig 19 (b)) during the normal and faulty condition is shown in Fig. 19 (d). I_1, I_2, and I_3 current passing through B_1, B_2, and B_3, respectively. I_{Total} is a total current of the HCB. In the normal mode, the current flows through B_1 that includes the fast mechanical switch and the commutation circuit. While the fault happens, turn-on and turn-off signals are sent to the commutation circuit and MB, respectively. After a time interval of T_1, the commutation circuit is switched OFF, and the current is commutated from B_1 to B_2 during T_2. Once the current commutation process finishes, the contacts of the MS start to open without arcing. After T_3, the distance between MS contacts is sufficient enough to endure the transient recovery voltage, and therefore the MS is turned off. Finally, the fault current commutates to the MOV and decreases to zero after T_4.

According to the structure of the HCB, the switching speed highly depends on mechanical parts. As a result, instead of the standard mechanical switch, a fast-acting mechanical switch that has to operate in less than 1 ms is needed [55],[98]. Besides having fast opening operation, the desired mechanical switch must have low conduction loss when carrying current, and high arc voltage [98].

4) *Z-source Circuit Breaker*

Generally, conventional SSCBs use an auxiliary circuit to push the current to zero by means of zero voltage switching or zero current switching to avoid any arc. However, the auxiliary device must actively be ready to reversely bias the main switch before that the fault current exceeds the interrupt capability of the breaker. Hence, strict fault detection and timing is a critical issue for conventional SSCBs.

Recently, a creatively designed ZSCB promises to mitigate this problem [99]. Although this class is developed form of the SSCB, according to its unique features including natural commutation, automatic disconnection of faulty load, simple control circuit, isolation from the fault to the source, inherent coordination capability, fault limiting capability by z-source impedance, and bidirectional power capability, this paper considers this type of the CB a separate class of the DCCB.

The main idea of the ZSCB is to take a part of large transient fault current and pass it through the Z-source capacitors to force the current of a Silicon-Controlled Rectifier (SCR) to approach zero, and therefore results in the SCR to commute off naturally. The scheme of the original ZSCB is shown in Fig. 20 (a). According to this structure, once the fault occurs, as the current

This article has been accepted for publication in a future issue of this journal, but has not been fully edited. Content may change prior to final publication. Citation information: DOI 10.1109/JESTPE.2019.2904588, IEEE Journal of Emerging and Selected Topics in Power Electronics

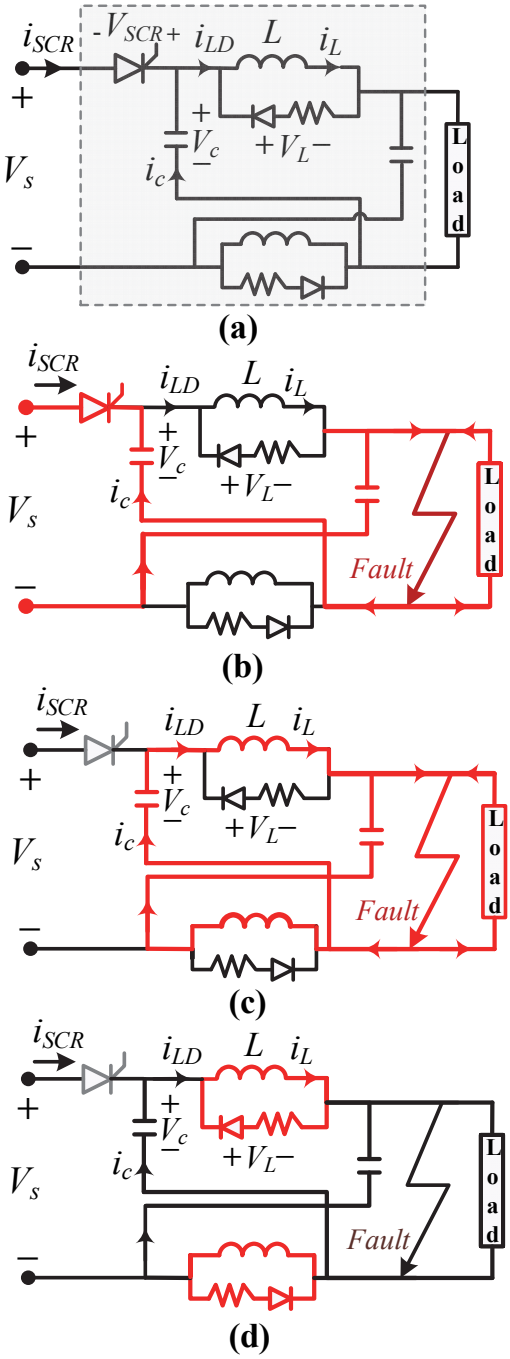

Fig. 20. (a) Scheme of the classical ZCB, (b) fault path during stage 1, (c) fault path during stage 2, (d) fault path during stage 3.

of the inductor is constant the fault current flows through the capacitors [see Fig. 20(b)]. In this stage, each of the capacitor current increases to reach the inductor current. At this stage, the i_{SCR} becomes zero and causes the SCR to commute off. A simple control circuit is also required to identify that the SCR has commuted off and then the gate voltage is removed from the SCR. In the next stage, the SCR is switched off and the two-series LC branches connected to the fault and load [see Fig. 20(c)]. These circuits start a resonance until the inductor voltage goes negative. At this point, the third stage starts and diodes turn ON to move away current from the capacitor. The capacitors current decay very fast and the inductor current will circulate in the inductor/resistor/diode loop until it approaches zero [see Fig. 20(d)]. Although the original z-source CB has abovementioned benefits, this CB cannot operate for less severe and lower dynamic fault because the current is not sufficiently high to naturally commute the ZSCB. In addition to this disadvantage, then there is no common ground between source and load, undesirable frequency response, high spike current during the reconnection, and not having bidirectional operation capability [100], [101],[102].

To address above-mentioned issued, various ZSCBs topologies have been proposed to deal with these issues [100]-[103]. Parallel-connected ZSCB, which is shown in Fig. 21(a), has a common ground connection between the source and all loads [104]. However, when the fault occurs, the source has a sum of inductor and capacitor current. As a result, the transient fault current is reflected in the source. Due to this disadvantage, an additional input filter is required. As shown in Fig. 21(b), the series-connected ZSCB, a shunt capacitor is used to intentionally divert the transient fault current from the source. This type of ZSCB also has a common ground connection, filtering capability at high frequency, and the reflected fault transient current to the source is significantly reduced [100]. However, in this topology, there is no isolation between source and faulty point while the SCR is turned off. In addition, if the load is purely resistive and a step change in load is greater than steady-state current, the SCR in all of the classical, parallel-connection, and series connection ZSCB will approach zero, and the breaker would turn off. To deal with such a step change in pure resistive load, a modified series-connected ZSCB is proposed [see Fig. 21(c)] [105]. In this topology, resistors in series are used to limit the transient current in the capacitors and allow step changes in load. In a DC microgrid with multiple energy sources, the power flow is bidirectional, due to this fact the implemented DCCBs must have the bidirectional capability. All of the original, parallel-connection and series-connection ZSCBs have to capability bidirectional operation. Two bidirectional ZSCBs based on the original ZSCB has been proposed [see Fig. 21(d) and (e)] [102]. The main disadvantages of both topologies are a high reflection of fault current to the source and lack of common ground between the DC source and load. Furthermore, since back-to-back SCRs require several independent drivers, the ZSCB cost will get higher. In [106], a bidirectional ZSCB that has a combination characteristics of series-connection and parallel connection- ZSCBs is proposed [see Fig. 21(f)] [106]. This ZSCB has superior features such as being reliable, cost-efficient, common ground between the DC source and load. However, a portion of the fault current is reflected in the source.

Recently, coupled inductors are integrated into designing the ZSCBs to reduce numbers of components, size, and weight. In [107], a new coupled inductor circuit breaker is introduced to attain the above-mentioned characteristics [see Fig. 21(g)]. This class of ZSCB has several advantages over original, parallel, series, and modified series ZSCBs such as being robust against the large load step change, having a common ground between source and load, and isolation of the source from the faulty point. Bidirectional operation capability is a needed

This article has been accepted for publication in a future issue of this journal, but has not been fully edited. Content may change prior to final publication. Citation information: DOI 10.1109/JESTPE.2019.2904588, IEEE Journal of Emerging and Selected Topics in Power Electronics

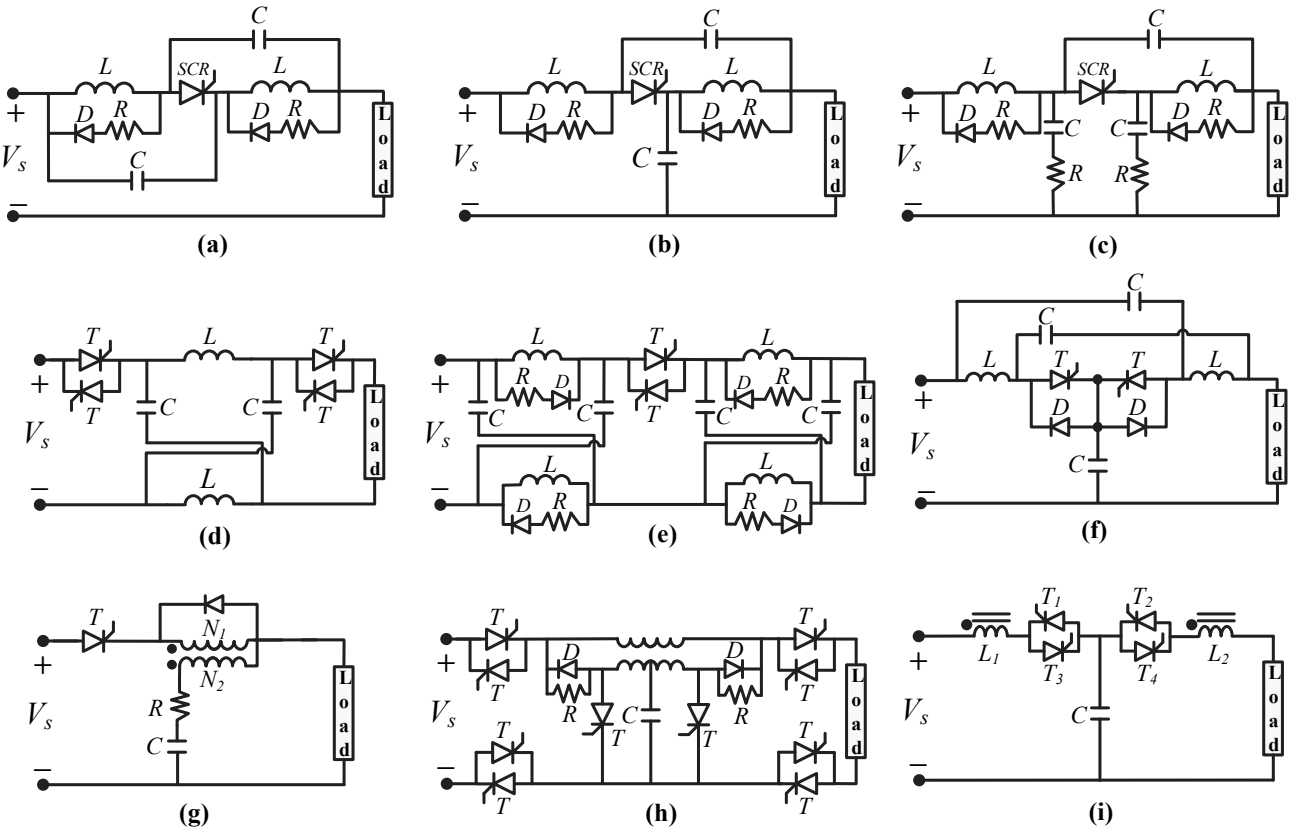

Fig. 21. ZSCB topology. (a) Parallel-connected ZSCB [104]. (b) Series-connected ZSCB [100], (c) A modified series-connected ZSCB [105]. (d) Bidirectional ZSCB (version1) [102], (e) Bidirectional ZSCB (version2) [102]. (f) Bidirectional ZSCB [106]. (g) Coupled-Inductor ZSCB [107]. (h) Bidirectional ZSCB [108]. (i) Bidirectional ZSCB [103].

TABLE IV. PROTECTIVE DEVICES USED IN DC MICROGRIDS.

Protective device	Disadvantages	Advantages
Fuse	• Not able to distinguish between a transient and a permanent fault • Fuse needs to be replaced for a successful operation	• Low cost • Simple structure
Mechanical circuit breaker	• †Long operating time (30-100 ms) • Limited interruption current capability	• Relatively low cost • Very low power loss
Solid state circuit breaker	• Expensive • High power loss • Big due to heatsink needed	• Fastest response time (<100μs) • Very long interruption lifetime
Hybrid circuit breaker	• Very expensive	• Low power loss • No arcing on mechanical contacts • Fast response time (Few ms)
Z-source circuit breaker	• A large transient fault is required to let ZSCB be activated. • ZSCB could not provide prolonged protection	• Natural commutation for critical fault • Lower cost than SSCBs

† MCB based on Thomson coil actuator could have time response between 1-3 m

feature to make such a ZSCB more applicable. In [108], a bidirectional coupled-inductor ZSCB is proposed based on a center-tapped transformer and bidirectional SCRs [see Fig. 21(h)]. Another type of bidirectional coupled-inductor ZSCB is proposed [see Fig. 21(i)] [103]. Suppose a conduction path is from source to load through L_1 and L_2, and T_3 and T_4. Then, a fault occurs in the DC load. In this case, the capacitor starts discharging through T_4 and L_2. Since, L_1 and L_2 are wound on the same core, a sudden increase in L_2 current leads to reverse current flow in L_1; therefore, the current in this inductor and T_3 approaches zero. Finally, T_3 turns off. While T_3 is disconnected, the C-L_2 circuit starts a resonance. After a while, T_4 voltage goes negative and at this moment the gate pulse is removed, and T_4 is tuned-off. Due to the absence of the freewheeling diodes across the inductors, voltage across the SCRs are higher. Therefore, the voltage rating of these devices must be selected carefully. In addition, since the capacitor voltage will be negative after the isolation process, a recharging circuit is required for re-breaking operation.

This article has been accepted for publication in a future issue of this journal, but has not been fully edited. Content may change prior to final publication. Citation information: DOI 10.1109/JESTPE.2019.2904588, IEEE Journal of Emerging and Selected Topics in Power Electronics

Table IV presents the advantages and disadvantages of each class of PDs. As a result, based on nominal voltage and current of the system, budget, acceptable complexity, time response, acceptable power loss, and demanded reliability, one of the protective device classes is chosen.

B. Breaker-less Protection

A "Breaker-less" approach to fault mitigation eliminates the need of DCCBs by using fully controllable power converters that coordinate with no load contactors or segmenting contactors to isolate fault [9], [109]-[110]. "Breaker-less" protection is also closely tied to the architectural implementation of the DC distribution system in order to minimize the loss of power to unfaulted parts of the system during potentially long fault isolation and recovery sequences. As shown in Fig. 22, this idea constitutes of four main stages [111], [112].

1. Once the fault occurs, the fault has to be detected and located.
2. Power converter(s) limit their current, driving current to zero and de-energizing the system at any output port affected by the fault
3. Power converter(s) coordinate the opening of appropriate contractors to isolate the faulty section
4. After isolation of the faulty section, the power converter(s) re-energize the system and return it to pre-faulted conditions.

Since the DCCBs are taken out of the DC system, one important constraint, or limitation, to "breaker-less" approaches is that the power converters must have fault current limiting capability under the conditions of short-circuited or near-short-circuited output. Some of the power converters do not have such a capability. For example, the commonly used VSC-based active rectifier has no control over its output current. For AC-fed DC systems, the following power converter topologies have inherent fault current limiting capability under output short circuit conditions: Thyristor–based phase-controlled rectifiers, Current-Source-Converter (CSC)-based active rectifiers, full bridge modular multilevel converters and passive rectifier fed DC-DC Buck Converters. For DC-fed DC systems, isolated DC-DC converters, current-fed DABs, buck DC-DC converters, and buck-boost DC-DC converters are well-suited for "breaker-less" approaches. A potential disadvantage of this method is increased complexity associated with fault detection , location, and the need to coordinate between multiple converters and isolating switches connected into a common faulted DC bus. Such approaches often rely heavily on centralized communication and the ability to isolate the fault is degraded when communication links fail. Also, the amount of time it takes to isolate the fault and restore the system is typically higher than what is achievable with "breaker-based" approaches.

VII. DC Fault Location Methods

As discussed in Section IV, the location of the fault must be identified precisely and quickly to help the repair crew to restore the faulty segment in a short time and to guarantee high microgrid reliability. Fault location methods are generally

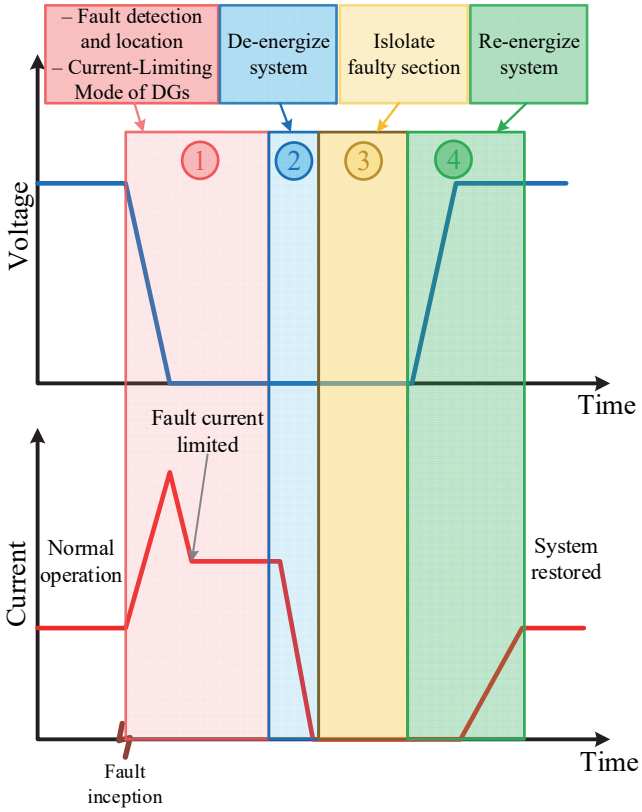

Fig. 22. Conceptual view of protection sequence in MVDC system.

classified into passive and active approaches. In the passive approach, including Traveling Wave (TW), differential, and local measurement, the fault location is determined based on existing signals. The main advantage of these methods is no requirement for an additional device to locate the exact fault position. On the other hand, inactive methods, use an external device to inject signals to locate fault. The main advantage of these methods is high accuracy regardless of the microgrid topology.

A. Travelling Wave Based Fault Location

Once a fault occurs, the initiated voltage and current traveling waves (TWs) propagate through the DC microgrid. According to this fact, the fault location can be identified by analyzing the traveling waves' features such as interval times at different locations [113], subsequent arrival times at one terminal [114], time difference between the first arriving waves at both terminals [115], and measurement of first arrival times of TWs at the converter stations [116]. However, TW-based fault location requires high-performance data acquisition equipment. In addition, in a microgrid with short distribution lines and a complex topology, many reflections happen, which has adverse effects on accuracy, and the surge arrivals time is low, which demands high sampling time. As a result, for such a microgrid the TW-based fault location is not a practical solution.

B. Differential Fault Location

Generally, the differential protection system is used for fault detection and relay operation. However, a few papers focus on fault location based on differential protection. In [117], current is measured from both sides of the line. These measured data is transferred through an Ethernet cable (IEC 61850) to either sides. In the first step, a number of differential current samples are considered for fault identification by the modified cumulative sum average method. Then, a set of samples including currents and voltages of both sides are taken and fed into non-iterative Moore-Penrose pseudo-inverse technique to calculate resistance and impedance from one side to the faulty point. Similar to the differential based fault detection methods, the main drawback of the differential based fault location methods is their dependency on the existence of the fast reliable communication systems.

C. Local Measurement Based Fault Location

This communication-free method operates based on measuring the local electrical variables and using them to calculate the fault distance. In [20], fault location is estimated by an iterative method using measuring voltage across a known length of the line. However, this method requires an additional voltage sensor and the fault distance error increases significantly with higher fault impedance. Another method is estimating the equivalent inductance between a PD and a fault to determine the faulty point. One of the main advantages of this method is being less affected by unknown fault resistance. In [118], local voltage, current, and *di/dt signals* are measured at each PDs to estimate inductance between the PD and the fault. The inductance is estimated from data samples at different time instants using online moving window least squares method. Fast *di/dt* increases the accuracy of fault location but makes it very sensitive to noise. As a result, an advanced digital *di*/*dt* calculation method and a well-designed digital filter are necessary for having a desired accuracy. In addition, this method is based on the dc microgrid in which a capacitor is only connected at one end of the cable, which is not the case in dc microgrid. This problem is addressed in [119] by driving a mathematical model of the faulty cable regarding capacitance connected at both ends of the cable. Then, the model is used along with the local measurement to determine the fault location. Another fault location method is based on the concept of the ratio of transient voltage, which is defined as the ratio of voltages measured at both sides of the inductor terminal in the time domain [120]. This method has two types including a single terminal and two terminals fault location. The former approach uses local measurement but it has low accuracy when fault resistance is high. On the other hand, the latter approach has higher accuracy at the expense of adding a communication system as well as two additional voltage sensors.

D. Injection Based Fault Location

Active impedance estimation (AIE) and power probe unit (PPU) based methods are two main types of injection-based fault location method. In the AIE based fault location method, a power converter is used to inject a triangle current waveform once the faulty conditions are identified, and then the impedance is calculated at the point of coupling. Finally, the reactive component is used to determine the fault location [121],[122],[123]. Another approach is using a probe power unit (PPU) to form a second-order RCL circuit through the fault path. Then, probe current response is analyzed, and the fault distance is obtained in term of damped resonant frequency [124],[125]. The main advantages of these two type of methods are no requirement for using communication system and high accuracy; however, since due to the need of additional equipment, the implementation cost is high.

VIII. Conclusion and Future Trends

According to the distinct characteristics of DC microgrids during fault scenarios, a proper protection system must be a key consideration. Systematic considerations, such as grid topology, grounding and interactions between inter-connected converters during fault events must be included as an integral part of the system design process. The fault current characteristic itself further complicates the issues—as the behavior is very dependent upon the power electronic converters connected into the system and the interconnecting cabling between them. As a result, with all of the operational benefits and potential benefits the DC microgrid brings when compared to AC microgrid, the system cannot be simply overlaid upon an existing protective infrastructure—as is perceived to be the case with AC microgrids. Protection has to be a part of the DC microgrid system design. While this fact appears to be a detriment, if in fact DC microgrid protection is an integral part of the DC microgrid system design, proper implementations may be discovered that make the DC microgrid even more applicable for wide range of applications. For example, although it was beyond the scope of this paper to describe the challenges associated with the protection of AC microgrids, it may very well be the case that, eventually, more resilient systems can be achieved that are DC if the current limiting capabilities of inter-connected power electronic converters that make up the DC microgrids are properly exploited.

From the standpoint of understanding the challenges associated with DC microgrid protection, this paper first investigates the DC fault current in three stages including the capacitor discharge stage, the freewheeling diodes stage, and the grid-side current feeding stage. In addition, the behavior of different topologies of non-isolated and isolated DC-DC converters has been investigated. Boost DC-DC converter is vulnerable to the short circuit fault, but other types of DC-DC converters such as buck, full-bridge, and DAB converters have some sort of fault current limiting capability. Among them, DAB converter can be a popular solution in DC microgrids as it provides bidirectional power flow that is demanding in future distributed applications with inherent electrical isolation and current limiting capability that are crucial for the electric system. Regarding the current limiting capability, in order to design a proper fault tolerant DC-DC converter, different characteristics such as power density, efficiency, fault current limiting, redundancy, and the cost have to be considered to meet the DC microgrid requirements.

The type of grounding system could also affect safety, the ability to identify the fault, and survivability of DC microgrid

under faulty conditions. Regarding these five grounding systems including TT, TN-S, TN-C. T-N-C-S, and IT; as well as six types of the grounding strategies including ungrounded, solidly grounded, grounded with a resistor, grounded with parallel resistors, diode grounded, and thyristor grounded systems are discussed and compared. According to this investigation, to have a better performance, a grounding system with a mixed configuration or more active components has to be considered.

This paper also reviews different methods of fault detection, isolation, and location. Five main DC fault detection methods including overcurrent protection, current derivative protection, directional overcurrent protection, differential protection, and distance protection. Each method has its own advantages and disadvantages. Most of the proposed methods are applied for low fault impedance, radial DC system, grounded system. However, for example, it is very hard to detect a high impedance fault in a multi-looped ungrounded DC microgrid. As a result, in order to detect the fault and coordinate the relays in such a DC microgrid, it is required to design a new fault detection and coordination algorithm that is independent of sensor error, communication system, or at least communication delay.

Since the nature of DC fault current is different from the ac one, protective devices that are utilized for "breaker-based" protective approaches must be designed to comply with the requirements. Five classes of fault isolation devices including fuses, MCBs, SSCBs, HCBs, and ZSCBs have been presented and compared in terms of cost, time response, power losses, and size. MCB has a very low power loss and longtime response; however, SSCB has high power loss and very fast time response. To have a protective device with fast response and low power loss, two classes of protective devices is combined to build a new class of isolation device so-called HCB. Recently, many developments in ultra-fast-acting mechanical circuit breaker, designing advanced commutation circuit, and integrating fault current limiter to the HCB are carried out to decrease cost, increase time response, and reduce the size of the HCB. Another promising solution is to employ the WBG materials such as SiC and GaN in the conventional SSCB to obtain much lower power loss and higher voltage, temperature, and frequency capabilities, thus reducing the complexity of the SSCB implementation.

In the final part of the review paper, two main types of fault location methods including passive and active have been discussed. Generally, the active fault location methods have high precision and fast time response, at the expense of an adding external device, and therefore high implemental cost.

Recently, a significant effort also has been devoted to the integration of fault detection, isolation, and location in device, so-called "breaker-less" protection. "Breaker-less" schemes impose constraints on the power converter topologies that are applied to the DC system, have characteristically more complex inter-communication requirements and longer recoverability time. Depending upon the distribution architecture, "breaker-less" protection may require redundant feeds to loads on common buses, bus partitioning and local energy storage because the faulted bus condition typically persists for a longer time when compared implementations that utilize DCCBs.

ACKNOWLEDGMENT

This work was supported in part by the National Science Foundation, grant no. 1439700, USA.

REFERENCES

[1] F. Wang, Y. Pei, D. Boroyevich, R. Burgos, and K. Ngo, "Ac vs . Dc Distribution for Off-Shore Power Delivery," in 34th Annual Conference of IEEE Industrial Electronics (IECON), 2018, pp. 2113–2118.

[2] E. Rodriguez-diaz, J. C. Vasquez, and J. M. Guerrero, "Intelligent DC homes in future sustainable energy systems: When efficiency and intelligence work together," IEEE Consum. Electron. Mag., vol. 5, no. 1, pp. 74–80, 2016.

[3] W. Lu and B.-T. Ooi, "Optimal acquisition and aggregation of offshore wind power by multiterminal voltage source HVDC," IEEE Trans. Power Deliv., vol. 18, no. 1, pp. 201–206, 2003.

[4] D. Jovcic, M. Taherbaneh, J. Taisne, and S. Nguefeu, "Offshore DC grids as an interconnection of radial systems: protection and control aspects," IEEE Trans. Smart Grid, vol. 6, no. 2, pp. 903–910, 2015.

[5] Z. Jin, G. Sulligoi, R. Cuzner, L. Meng, J. C. Vasquez, and J. M. Guerrero, "Next-Generation shipboard DC power system: Introduction smart grid and dc microgrid technologies into maritime electrical netowrks," IEEE Electrif. Mag., vol. 4, no. 2, pp. 45–57, 2016.

[6] A. Emadi, S. S. Williamson, and A. Khaligh, "Power electronics intensive solutions for advanced electric, hybrid electric, and fuel cell vehicular power systems," IEEE Trans. Power Electron., vol. 21, no. 3, pp. 567–577, 2006.

[7] P. A. Madduri, J. Rosa, S. R. Sanders, E. A. Brewer, and M. Podolsky, "Design and verification of smart and scalable DC microgrids for emerging regions," in IEEE Energy Conversion Congress and Exposition, 2013, pp. 73–79.

[8] A. Jhunjhunwala, A. Lolla, and P. Kaur, "Solar-dc microgrid for Indian homes: A transforming power scenario," IEEE Electrif. Mag., vol. 4, no. 2, pp. 10–19, 2016.

[9] R. M. Cuzner and G. Venkataramanan, "The status of DC micro-grid protection," in Industry Applications Society Annual Meeting, 2008, pp. 1–8.

[10] R. M. Cuzner, K. Palaniappan, W. Sedano, N. Hoeft, and Mengyuan Qi, "Fault characterization and protective system design for a residential DC microgrid," in IEEE 6th International Conference on Renewable Energy Research and Applications (ICRERA), 2017, pp. 642–647.

[11] M. Mobarrez, D. Fregosi, S. Bhattacharya, and N. Carolina, "Grounding Architectures for Enabling Ground Fault Ride-Through Capability in DC Microgrids," in International Conference on DC Microgrids (ICDCM), 2017, pp. 81–87.

[12] K. Palaniappan, W. Sedano, N. Hoeft, R. Cuzner, and Z. J. Shen, "Fault discrimination using SiC JFET based self- powered solid state circuit breakers in a residential DC community microgrid," in IEEE Energy Conversion Congress and Exposition (ECCE), 2017, pp. 3747–3753.

[13] Z. J. Shen, G. Sabui, Z. Miao, and Z. Shuai, "Wide-Bandgap Solid-State Circuit Breakers for DC Power Systems : Device and Circuit Considerations," IEEE Trans. Electron Devices, vol. 62, no. 2, pp. 294–300, 2015.

[14] T. Dragičević, X. Lu, J. C. Vasquez, and J. M. Guerrero, "DC Microgrids-Part II: A Review of Power Architectures, Applications, and Standardization Issues," IEEE Trans. Power Electron., vol. 31, no. 5, pp. 3528–3549, 2016.

[15] IEC. 60364-1, "IEC 60364-1 Low-Voltage Electrical Installations—Part 1: Fundamental Principles, Assessment of General Characteristics, Definition," vol. 11, 2005.

[16] S. D. A. Fletcher, P. J. Norman, S. J. Galloway, and G. M. Burt, "Determination of protection system requirements for DC unmanned aerial vehicle electrical power networks for enhanced capability and survivability," IET Electr. Syst. Transp., vol. 1, no. 4, pp. 137–147, 2011.

[17] F. Wang, Z. Lei, X. Xu, and X. Shu, "Topology deduction and

analysis of voltage balancers for DC microgrid," IEEE J. Emerg. Sel. Top. Power Electron., vol. 5, no. 2, pp. 672–680, 2017.

[18] D. Salomonsson, S. Member, L. Söder, and A. Sannino, "Protection of Low-Voltage DC Microgrids," IEEE Trans. Power Del., vol. 24, no. 3, pp. 1045–1053, 2009.

[19] R. Cuzner and A. Jeutter, "DC zonal electrical system fault isolation and reconfiguration," in IEEE Electric Ship Technologies Symposium, 2009, pp. 227–234.

[20] J. Yang, J. E. Fletcher, J. O. Reilly, and S. Member, "Short-Circuit and Ground Fault Analyses and Location in VSC-Based DC Network Cables," IEEE Trans. Ind. Electron., vol. 59, no. 10, pp. 3827–3837, 2012.

[21] R. M. Cuzner, T. Sielicki, A. E. Archibald, and D. A. McFarlin, "Management of ground faults in an ungrounded multi-terminal zonal DC distribution system with auctioneered loads," in IEEE Electric Ship Technologies Symposium, 2011, pp. 300–305.

[22] R. M. Cuzner et al., "Considerations when diode auctioneering multiple DC buses in a non-isolated DC distribution system," in IEEE Electric Ship Technologies Symposium, 2011, pp. 277–282.

[23] L. Qi, A. Antoniazzi, and L. Raciti, "DC Distribution Fault Analysis, Protection Solutions, and Example Implementations," IEEE Trans. Ind. Appl., vol. 54, no. 4, pp. 3179–3186, 2018.

[24] M. Shahbazi, E. Jamshidpour, P. Poure, S. Saadate, and M. R. Zolghadri, "Open- and Short-Circuit Switch Fault Diagnosis for Nonisolated DC–DC Converters Using Field Programmable Gate Array," IEEE Trans. Ind. Electron., vol. 60, no. 9, pp. 4136–4146, 2013.

[25] Z. Xiao, "An Instantaneously Triggered Short-Circuit Protection Architecture for Boost Switching DC/DC Converters," IEEE Trans. Power Electron., vol. 33, no. 7, pp. 5677–5685, 2018.

[26] Shulin Liu ; Jian Liu ; Yinling Yang ; Jiuming Zhong, "Design of intrinsically safe buck DC/DC converters," in International Conference on Electrical Machines and Systems, 2005.

[27] Y. A. Harrye, K. H. Ahmed, and A. A. Aboushady, "DC fault isolation study of bidirectional dual active bridge DC/DC converter for DC transmission grid application," in 41st Annual Conference of the IEEE Industrial Electronics Society, 2015, pp. 3193–3198.

[28] R. Zhou, H. S.-H. Chung, R. Z. R. Zhou, H. S.-H. Chung, and R. Zhang, "Inductive power transfer system for driving multiple OLED lighting panels," IEEE Trans. Power Electron., vol. 31, no. 10, pp. 7131–7147, 2016.

[29] M. I. Rahman, K. H. Ahmed, and D. Jovcic, "Analysis of DC Fault for Dual Active Bridge DC/DC Converter including Prototype Verification," IEEE J. Emerg. Sel. Top. Power Electron., p. (early access), 2018.

[30] P. Cairoli, R. Rodrigues, and Huaxi Zheng, "Fault Current Limiting Power Converters for Protection of DC Microgrids," in SoutheastCon, 2017.

[31] H. Liu, Y. Ji, L. Wang, and P. Wheeler, "A family of improved magnetically coupled impedance network boost DC-DC converters," IEEE Trans. Power Electron., vol. 33, no. 5, pp. 3697–3702, 2018.

[32] D. Cao and F. Z. Peng, "A Family of Z-source and Quasi-Z-source DC-DC Converters," in 2009 Twenty-Fourth Annual IEEE Applied Power Electronics Conference and Exposition, 2009, pp. 1097–1101.

[33] D. Paul, "DC traction power system grounding," IEEE Trans. Ind. Appl., vol. 38, no. 3, pp. 818–824, 2002.

[34] J. Do Park and J. Candelaria, "Fault detection and isolation in low-voltage dc-bus microgrid system," IEEE Trans. Power Deliv., vol. 28, no. 2, pp. 779–787, 2013.

[35] J. Mohammadi, F. B. Ajaei, and G. Stevens, "DC microgrid grounding strategies," in IAS 54th Industrial and Commercial Power Systems Technical Conference (I&CPS), 2018, pp. 1–6.

[36] "Electrical installation guide According to IEC international," 2013.

[37] M. Mitolo, "Of electrical distribution systems with multiple grounded neutrals," IEEE Trans. Ind. Appl., vol. 46, no. 4, pp. 1541–1546, 2010.

[38] J. Dentler and K. Pettersen, "Distribution and grounding issues involved in naval ship integration of an electric gun system," IEEE Trans. Magn., vol. 29, no. 1, pp. 929–933, 1993.

[39] Y. Wang, Z. Yu, J. He, S. Chen, R. Zeng, and B. Zhang, "Performance of shipboard medium-voltage DC system of various grounding modes under monopole ground fault," IEEE Trans. Ind. Appl., vol. 51, no. 6, pp. 5002–5009, 2015.

[40] E. Baran and R. Mahajan, "Overcurrent Protection on Voltage-Source-Converter- Based Multiterminal DC Distribution Systems," IEEE Trans. Power Deliv., vol. 22, no. 1, pp. 406–412, 2007.

[41] M. Monadi, C. Koch-ciobotaru, A. Luna, J. I. Candela, and P. Rodriguez, "A Protection Strategy for Fault Detection and Location for Multi-Terminal MVDC Distribution Systems with Renewable Energy Systems," in International Conference on Renewable Energy Research and Application (ICRERA), 2014, pp. 496–501.

[42] S. D. A. Fletcher, P. J. Norman, S. J. Galloway, P. Crolla, and G. M. Burt, "Optimizing the roles of unit and non-unit protection methods within DC microgrids," IEEE Trans. Smart Grid, vol. 3, no. 4, pp. 2079–2087, 2012.

[43] K. A. Saleh, A. Hooshyar, and E. F. El-Saadany, "Hybrid Passive-Overcurrent Relay for Detection of Faults in Low-Voltage DC Grids," IEEE Trans. Smart Grid, pp. 1–10, 2015.

[44] A. Meghwani, S. C. Srivastava, and S. Chakrabarti, "A Non-unit Protection Scheme for DC Microgrid Based on Local Measurements," IEEE Trans. Power Deliv., vol. 32, no. 1, pp. 172–181, 2017.

[45] A. A. S. Emhemed and G. M. Burt, "An advanced protection scheme for enabling an LVDC last mile distribution network," IEEE Trans. Smart Grid, vol. 5, no. 5, pp. 2602–2609, 2014.

[46] A. A. S. Emhemed, K. Fong, S. Fletcher, and G. M. Burt, "Validation of fast and selective protection scheme for an LVDC distribution network," IEEE Trans. Power Deliv., vol. 32, no. 3, pp. 1432–1440, 2017.

[47] P. Cairoli and R. A. Dougal, "Fault detection and isolation in medium-voltage DC microgrids: Coordination between supply power converters and bus contactors," IEEE Trans. Power Electron., vol. 33, no. 5, pp. 4535–4546, 2018.

[48] A. Meghwani, S. C. Srivastava, and S. Chakrabarti, "A New Protection Scheme for DC Microgrid using Line Current Derivative," in 2015 IEEE Power & Energy Society General Meeting, 2015, pp. 1–5.

[49] S. D. A. Fletcher, P. J. Norman, K. Fong, S. J. Galloway, and G. M. Burt, "High-speed differential protection for smart DC distribution systems," IEEE Trans. Smart Grid, vol. 5, no. 5, pp. 2610–2617, 2014.

[50] C. Yuan, M. a. Haj-ahmed, and M. Illindala, "Protection Strategies for Medium Voltage Direct Current Microgrid at a Remote Area Mine Site," IEEE Trans. Ind. Appl., vol. 9994, no. c, pp. 1–1, 2015.

[51] L. Tang and B. T. Ooi, "Locating and isolating DC faults in multi-terminal DC systems," IEEE Trans. Power Deliv., vol. 22, no. 3, pp. 1877–1884, 2007.

[52] H. Zhan et al., "Placement and Sizing of Distributed Generation Sources in Distribution Networks," vol. 7, no. 1, pp. 1–11, 2015.

[53] J. P. Brozek, "DC overcurrent protection-where we stand," IEEE Trans. Ind. Appl., vol. 29, no. 5, pp. 1029–1032, 1993.

[54] R. Cuzner, D. Macfarlin, D. Clinger, M. Rumney, and G. Castles, "Circuit Breaker Protection Considerations in Power Converter-Fed DC Systems," in Electric Ship Technologies Symposium, 2009, pp. 360–367.

[55] C. Meyer, M. Kowal, and R. W. De Doncker, "Circuit breaker concepts for future high-power DC-applications," in Conference Record - IAS Annual Meeting (IEEE Industry Applications Society), 2005, pp. 860–866.

[56] M. Kuzuhara and H. Tokuda, "Low-loss and high-voltage III-nitride transistors for power switching applications," IEEE Trans. Electron Devices, vol. 62, no. 2, pp. 405–413, 2015.

[57] Z. J. Shen, Z. Miao, and A. M. Roshandeh, "Solid State Circuit Breakers for DC Micrgrids: Current Status and Future Trends," in International Conference on DC Microgrids (ICDCM), 2015, pp. 228–233.

[58] J. Häfner and B. Jacobson, "Proactive Hybrid HVDC Breakers - A key innovation for reliable HVDC grids," in Cigre symposium, 2011, pp. 1–8.

[59] A. Shukla and G. D. Demetriades, "A Survey on Hybrid Circuit-

Breaker Topologies," IEEE Trans. Power Deliv., vol. 30, no. 2, pp. 627–641, 2015.

[60] PMS 320, "Naval Power Systems Technology Development Roadmap," 2013.

[61] B. R. Schmerda, R. Cuzner, R. Clark, and D. Nowak, "Shipboard Solid-State Protection: Overview and Applications," IEEE Electrif. Mag., vol. 1, no. 1, pp. 32–39, 2013.

[62] B. Z. J. Shen, "Ultrafast Solid-State Circuit Breakers: Protecting Converter-Based ac and dc Microgrids Against Short Circuit Faults," IEEE Electrif. Mag., vol. 4, no. 2, pp. 67–72, 2016.

[63] H. O. Brien, A. Ogunniyi, W. Shaheen, C. J. Scozzie, and V. Temple, "Development of SiC multi-chip module for pulse switching at 10 kV, 100 kA," in IEEE Pulsed Power Conference (PPC), 2015, pp. 1–5.

[64] B. R. Adapa, "High-Wire Act: HVdc Technology: The State of the Art," IEEE power energy Mag., no. October, pp. 18–29, 2012.

[65] H. Li, W. Li, M. Luo, A. Monti, and F. Ponci, "Design of smart MVDC power grid protection," IEEE Trans. Instrum. Meas., vol. 60, no. 9, pp. 3035–3046, 2011.

[66] K. Tahata et al., "HVDC circuit breakers for HVDC grid applications," in Proc. AORC-CIGRÉ, 2014, pp. 1–9.

[67] F. Wang, Z. Zhang, T. Ericsen, R. Raju, R. Burgos, and D. Boroyevich, "Advances in Power Conversion and Drives for Shipboard Systems," Proc. IEEE, vol. 103, no. 12, pp. 2285–2311, 2015.

[68] C. Meyer, S. Schröder, and R. W. De Doncker, "Solid-state circuit breakers and current limiters for medium-voltage systems having distributed power systems," IEEE Trans. Power Electron., vol. 19, no. 5, pp. 1333–1340, 2004.

[69] C. Meyer, M. Höing, and R. W. De Doncker, "Novel solid-state circuit breaker based on active thyristor topologies," PESC Rec. - IEEE Annu. Power Electron. Spec. Conf., vol. 4, no. 2, pp. 2559–2564, 2004.

[70] Z. Chen, Z. Yu, X. Zhang, T. Wei, G. Lyu, and L. Qu, "Analysis and Experiments for IGBT , IEGT , and IGCT in Hybrid DC Circuit Breaker," IEEE Trans. Ind. Electron., vol. 65, no. 4, pp. 2883–2892, 2018.

[71] J. Millan, P. Godignon, X. Perpina, A. Perez-Tomas, and J. Rebollo, "A Survey of Wide Bandgap Power Semiconductor Devices," IEEE Trans. Power Electron., vol. 29, no. 5, pp. 2155–2163, 2014.

[72] T. P. Chow, "Wide Bandgap Semiconductor Power Devices for Energy Efficient Systems," in in Proc. IEEE Workshop Wide Bandgap Power Devices Appl. (WiPDA), pp. 402–405.

[73] A. Lostetter et al., "High-temperature silicon carbide and silicon on insulator based integrated power modules," in Vehicle Power and Propulsion Conference, 2009, pp. 1032–1035.

[74] K. Sheng and S. Member, "Maximum Junction Temperatures of SiC Power Devices," IEEE Trans. Electron Devices, vol. 56, no. 2, pp. 337–342, 2009.

[75] T. Lebey, I. Omura, M. Kozako, H. Kawano, and M. Hikita, "High Temperature High Voltage Packaging of Wideband Gap Semiconductors Using Gas Insulating Medium," in International Power Electronics Conference, 2010, pp. 180–186.

[76] T. Funaki et al., "Power Conversion With SiC Devices at Extremely High Ambient Temperatures," IEEE trans. Power Elecron., vol. 22, no. 4, pp. 1321–1329, 2007.

[77] R. J. Kaplar, J. C. Neely, D. L. Huber, and L. J. Rashkin, "Generation-after-next power electronics: Ultrawide-bandgap devices, high-temperature packaging, and magnetic nanocomposite materials," IEEE Power Electron. Mag., vol. 4, no. 1, pp. 36–42, 2017.

[78] Alex Q. Huang, "Power Semiconductor Devices for Smart Grid and Renewable Energy Systems," Proc. IEEE, vol. 105, no. 11, pp. 2019–2047, 2019.

[79] J. L. Hudgins, S. Member, G. S. Simin, E. Santi, S. Member, and M. A. Khan, "An Assessment of Wide Bandgap Semiconductors for Power Devices," IEEE trans. Power Elecron., vol. 18, no. 3, pp. 907–914, 2003.

[80] E. T. E. T. O. Thyristor, X. Song, S. Member, A. Q. Huang, and M. Lee, "Theoretical and Experimental Study of 22 kV SiC," IEEE trans. Power Elecron., vol. 32, no. 8, pp. 6381–6393, 2017.

[81] L. Cheng et al., "Advanced Silicon Carbide Gate Turn-Off Thyristor for Energy Conversion and Power Grid Applications," in Energy Conversion Congress and Exposition (ECCE), 2012, pp. 2249–2252.

[82] T. Igbts, R. Withanage, and N. Shammas, "Series Connection of Insulated Gate Bipolar Transistors (IGBTs)," IEEE trans. Power Elecron., vol. 27, no. 4, pp. 2204–2212, 2012.

[83] X. She, A. Q. Huang, and B. Ozpineci, "Review of Silicon Carbide Power Devices and their applications," IEEE Trans. Ind. Electron., vol. 64, no. 10, pp. 8193–8205, 2017.

[84] K. Vechalapu et al., "Comparative Evaluation of 15-kV SiC MOSFET and 15-kV SiC IGBT for Medium-Voltage Converter Under the Same dv / dt Conditions," IEEE J. Emerg. Sel. Top. Power Electron., vol. 5, no. 1, pp. 469–489, 2017.

[85] B. Wrzecionko, S. Member, D. Bortis, and J. W. Kolar, "A 120 ◦ C Ambient Temperature Forced Air-Cooled Normally-off SiC JFET Automotive Inverter System," IEEE trans. Power Elecron., vol. 29, no. 5, pp. 2345–2358, 2014.

[86] D. Sadik et al., "Short-Circuit Protection Circuits for Silicon-Carbide Power Transistors," IEEE Trans. Ind. Electron., vol. 63, no. 4, pp. 1995–2004, 2016.

[87] D. Aggeler, F. Canales, J. Biela, and J. W. Kolar, "D v/D t-Control Methods for the SiC JFET/Si MOSFET Cascode," IEEE trans. Power Elecron., vol. 28, no. 8, pp. 4074–4082, 2013.

[88] Y. Tang et al., "Ultrahigh-Speed GaN High-Electron-Mobility Transistors With fT/f max of 454 / 444 GHz," ieee electron device Lett., vol. 36, no. 6, pp. 549–551, 2015.

[89] E. A. Jones, S. Member, F. F. Wang, and D. Costinett, "Review of Commercial GaN Power Devices and GaN-Based Converter Design Challenges," IEEE J. Emerg. Sel. Top. Power Electron., vol. 4, no. 3, pp. 707–719, 2016.

[90] U. K. Mishra, P. Parikh, and Y. Wu, "AlGaN/GaN HEMTs — An Overview of Device Operation and Applications," Proc. IEEE, vol. 90, no. 6, pp. 1022–1031, 2002.

[91] A. Hariya, S. Member, T. Koga, K. Matsuura, H. Yanagi, and S. Tomioka, "Circuit Design Techniques for Reducing the Effects of Magnetic Flux on GaN-HEMTs in 5-MHz 100-W High Power-Density LLC Resonant," IEEE trans. Power Elecron., vol. 32, no. 8, pp. 5953–5963, 2017.

[92] L. Zhang, R. Woodley, X. Song, S. Sen, X. Zhao, and A. Q. Huang, "High current medium voltage solid state circuit breaker using paralleled 15kV SiC ETO," in Conference Proceedings - IEEE Applied Power Electronics Conference and Exposition - APEC, 2018, vol. 2018–March, pp. 1706–1709.

[93] Y. Sato, Y. Tanaka, A. Fukui, M. Yamasaki, and H. Ohashi, "SiC-SIT circuit breakers with controllable interruption voltage for 400-V DC distribution systems," IEEE Trans. Power Electron., vol. 29, no. 5, pp. 2597–2605, 2014.

[94] F. F. Wang and Z. Zhang, "Overview of silicon carbide technology: Device, converter, system, and application," CPSS Trans. Power Electron. Appl., vol. 1, no. 1, pp. 13–32, 2016.

[95] N. Oswald, P. Anthony, N. McNeill, and B. H. Stark, "An experimental investigation of the tradeoff between switching losses and EMI generation with hard-switched All-Si, Si-SiC, and All-SiC device combinations," IEEE Trans. Power Electron., vol. 29, no. 5, pp. 2393–2407, 2014.

[96] C. Peng, A. Q. Huang, and X. Song, "Current commutation in a medium voltage hybrid DC circuit breaker using 15 kV vacuum switch and SiC devices," in Conference Proceedings - IEEE Applied Power Electronics Conference and Exposition - APEC, 2015, pp. 2244–2250.

[97] W. Wen, Y. Huang, Y. Sun, J. Wu, M. Al-dweikat, and W. Liu, "Research on Current Commutation Measures for Hybrid DC Circuit Breakers," IEEE Trans. Power Del., vol. 31, no. 4, pp. 1456–1463, 2016.

[98] C. Peng, I. Husain, A. Q. Huang, B. Lequesne, and R. Briggs, "A Fast Mechanical Switch for Medium-Voltage Hybrid DC and AC Circuit Breakers," IEEE Trans. Ind. Appl., vol. 52, no. 4, pp. 2911–2918, 2016.

[99] K. A. Corzine and R. W. Ashton, "A new Z-source DC circuit breaker," IEEE Trans. Power Electron., vol. 27, no. 6, pp. 2796–2804, 2012.

[100] A. H. Chang, B. R. Sennett, A. T. Avestruz, S. B. Leeb, and J. L. Kirtley, "Analysis and Design of DC System Protection Using Z-Source Circuit Breaker," IEEE Trans. Power Electron., vol. 31, no. 2, pp. 1036–1049, 2016.

[101] P. Prempraneerach, M. G. Angle, J. L. K. Jr, G. E. Karniadakis, and C. Chryssostomidis, "Optimization of a Z-Source DC Circuit Breaker," in IEEE Electric Ship Technologies Symposium (ESTS), 2013, pp. 480–486.

[102] A. Maqsood and K. Corzine, "The Z-Source Breaker for Fault Protection in Ship Power Systems," in International Symposium on Power Electronics, Electrical Drives, Automation and Motion, 2014, pp. 307–312.

[103] S. G. Savaliya and B. G. Fernandes, "Modified Bi-directional Z-Source Breaker with Reclosing and Rebreaking Capabilities," in IEEE Applied Power Electronics Conference and Exposition (APEC), 2018, pp. 3497–3504.

[104] K. A. Corzine and R. W. Ashton, "Structure and Analysis of the Z-Source MVDC Breaker," in IEEE Electric Ship Technologies Symposium, 2011, pp. 334–338.

[105] A. Maqsood, A. Overstreet, and K. A. Corzine, "Modified Z-Source DC Circuit Breaker Topologies," IEEE trans. Power Elecron., vol. 31, no. 10, pp. 7394–7403, 2016.

[106] D. Keshavarzi, T. Ghanbari, and E. Farjah, "A Z-Source-Based Bidirectional DC Circuit Breaker With Fault Current Limitation and Interruption Capabilities," IEEE trans. Power Elecron., vol. 32, no. 9, pp. 6813–6822, 2017.

[107] K. A. Corzine, "A New-Coupled-Inductor Circuit Breaker for DC Applications," IEEE trans. Power Elecron., vol. 32, no. 2, pp. 1411–1418, 2017.

[108] A. Maqsood and K. Corzine, "DC Microgrid Protection: Using the Coupled-Inductor Solid-State Circuit Breaker," IEEE Electrif. Mag., vol. 4, no. 2, pp. 58–64, 2016.

[109] P. Cairoli, S. Member, I. Kondratiev, S. Member, R. A. Dougal, and S. Member, "Coordinated Control of the Bus Tie Switches and Power Supply Converters for Fault Protection in DC Microgrids," IEEE Trans. Power Electron., vol. 28, no. 4, pp. 2037–2047, 2013.

[110] R. M. Cuzner and D. A. Esmaili, "Fault Tolerant Shipboard MVDC Architectures," in International Conference on Electrical Systems for Aircraft, Railway, Ship Propulsion and Road Vehicles (ESARS), 2015, pp. 1–6.

[111] B. P. Cairoli and R. A. Dougal, "New Horizons in DC Shipboard Power Systems," Electrif. Mag., vol. 1, no. december 2013, pp. 38–45, 2014.

[112] D. Soto, M. Sloderbeck, H. Ravindra, and M. Steurer, "Advances to Megawatt Scale Demonstrations of High Speed Fault Clearing and Power Restoration in Breakerless MVDC Shipboard Power Systems," in Electric Ship Technologies Symposium (ESTS), 2017, pp. 312–315.

[113] O. M. K. K. Nanayakkara, A. D. Rajapakse, and R. Wachal, "Location of DC line faults in conventional HVDC systems with segments of cables and overhead lines using terminal measurements," IEEE Trans. Power Deliv., vol. 27, no. 1, pp. 279–288, 2012.

[114] M. Ando, E. O. Schweitzer, and R. A. Baker, "Development and Field-Data Evaluation of Single-End Fault Locator for Two-Terminal HVDV Transmission Lines-Part 2 : Algorithm and Evaluation," Comput. Commun., vol. 2, no. 4, p. 187, 1979.

[115] M. B. Dewe, S. Sankar, and J. Arrillaga, "The application of satellite time references to HVDC fault location," IEEE Trans. Power Del., vol. 8, no. 3, pp. 1295–1302, 1993.

[116] S. Azizi, M. Sanaye-pasand, M. Abedini, and A. Hasani, "A Traveling-Wave-Based Methodology for Wide-Area Fault Location in Multiterminal DC Systems," Ieee Trans. Power Deliv., vol. 29, no. 6, pp. 2552–2560, 2014.

[117] S. Dhar, R. K. Patnaik, and P. K. Dash, "Fault Detection and Location of Photovoltaic Based DC Microgrid Using Differential Protection Strategy," IEEE Trans. Smart Grid, vol. 9, no. 5, pp. 4303–4312, 2018.

[118] X. Feng, L. Qi, and J. Pan, "A Novel Fault Location Method and Algorithm for DC Distribution Protection," IEEE Trans. Ind. Appl., vol. 53, no. 3, pp. 1834–1840, 2017.

[119] A. Meghwani, S. C. Srivastava, and S. Chakrabarti, "Local measurement-based technique for estimating fault location in multi-source DC microgrids," IET Gener. Transm. Distrib., vol. 12, no. 13, pp. 3305–3313, 2018.

[120] S. Jiang, C. Fan, N. Huang, Y. Zhu, and M. He, "A Fault Location Method for DC Lines Connected with DAB Terminal in Power Electronic Transformer," IEEE Trans. Power Deliv., vol. 34, no. 1, pp. 301–311, 2018.

[121] E. Christopher, M. Sumner, D. W. P. Thomas, X. Wang, and F. De Wildt, "Fault location in a zonal DC marine power system using active impedance estimation," IEEE Trans. Ind. Appl., vol. 49, no. 2, pp. 860–865, 2013.

[122] K. Jia, T. Bi, B. Liu, E. Christopher, D. W. P. Thomas, and M. Sumner, "Marine Power Distribution System Fault Location Using a Portable Injection Unit," IEEE Trans. Power Deliv., vol. 30, no. 2, pp. 818–826, 2015.

[123] K. Jia, E. Christopher, D. Thomas, M. Sumner, and T. Bi, "Advanced DC zonal marine power system protection," IET Gener. Transm. Distrib., vol. 8, no. 2, pp. 301–309, 2013.

[124] J. Do Park, J. Candelaria, L. Ma, and K. Dunn, "DC ring-bus microgrid fault protection and identification of fault location," IEEE Trans. Power Deliv., vol. 28, no. 4, pp. 2574–2584, 2013.

[125] R. Mohanty, U. S. M. Balaji, A. K. Pradhan, and S. Member, "An Accurate Noniterative Fault-Location Technique for Low-Voltage DC Microgrid," IEEE Trans. Power Del., vol. 31, no. 2, pp. 475–481, 2016.

Siavash Beheshtaein (S'12) was born in Shiraz, Iran, in 1986. He received the B.Sc. and M.Sc. degrees in electrical engineering from Shiraz University, Iran, in 2012 and 2014, respectively. He also received his Ph.D. degree from Aalborg University, Denmark, in 2018.

He is currently a postdoc fellow at the University of Wisconsin–Milwaukee, WI, USA. His research interests include microgrid protection, adaptive protection, wireless power transfer, solid-state transformer, and dc circuit breakers.

Robert Cuzner (M'90, SM'03) received the B.S.degree from Brigham Young University, Provo, UT, USA, and the M.S. and Ph.D. degrees from the University of Wisconsin–Madison, Madison, WI, USA, all in electrical and computer engineering. In 1990, his professional work began with Miller Electric Manufacturing Company, Appleton, WI, USA designing generators for engine-driven welders. He worked at Eaton Corporation, Milwaukee, WI, USA, from 1993 to 2002 and then DRS Power and Control Technologies, Inc., from 2002 to 2014 as a designer of power conversion systems for Navy shipboard applications. He is presently Associate Professor in the Department of Electrical Engineering and Computer Science at the University of Wisconsin–Milwaukee. Dr. Cuzner has over 25 years of experience working in power generation, power conversion, and drive system controls and packaging for both Navy and industrial applications. He has authored over 50 publications, including IEEE journal and conference papers and tutorials, and is the holder of three U.S. patents. His interests include microgrid protection, distributed generation, power electronics for power distribution and drive

systems, low- and medium-voltage power conversion system design, high power-density packaging of power electronics, and electric machine design.

Mojtaba Forouzesh (S'14) received the B.S. degree in Physics and the M.S. degree in Electrical Engineering (with highest honor) from the University of Guilan, Rasht, Iran, in 2011, and 2015, respectively. He is currently working toward the PhD degree at the Department of Electrical and Computer Engineering, Queen's University, Kingston, ON, Canada. From 2015 to 2018, he was working on several research studies as a Research Collaborator with the Department of Energy Technology, Aalborg University, Aalborg, Denmark. His research interests include dc-dc power conversion, PV inverters, high efficiency step-up/step-down converters using wide-bandgap semiconductors (i.e. SiC and GaN devices), small signal modeling of power converters, and digital implementation of modulation and control schemes.
Mr. Forouzesh is a member of the IEEE Power Electronics Society (PELS) and the Industrial Electronics Society, and a frequent reviewer for IEEE PELS sponsored conferences, and the *IEEE Transactions on Power Electronics*, the *IEEE Transactions on Industrial Electronics*, the *IEEE Journal of Emerging and Selected Topics in Power Electronics*, the *IET Power Electronics,* and the Wiley *International Journal of Circuit Theory and Applications*.

Mehdi Savaghebi (S'06-M'15-SM'15) was born in Karaj, Iran, in 1983. He received the B.Sc. degree from University of Tehran, Iran, in 2004 and the M.Sc. and Ph.D. degrees with highest honors from Iran University of Science and Technology, Tehran, Iran in 2006 and 2012, respectively, all in Electrical Engineering. From 2007 to 2014, he was a Lecturer in Electrical Engineering Department, Karaj Branch, Islamic Azad University. In 2010, he was a visiting Ph.D. Student with the Department of Energy Technology, Aalborg University, Aalborg, Denmark and with the Department of Automatic Control Systems and Computer Engineering, Technical University of Catalonia, Barcelona, Spain. From 2014 to 2017, he was a Postdoc Fellow in the Department of Energy Technology, Aalborg University where he was an Associate Professor for 2017-2018. Currently, he is an Associate Professor with Electrical Engineering Section, the Mads Clausen Institute, University of Southern Denmark, Odense, Denmark. His main research interests include distributed generation systems, microgrids, power quality and protection of electrical systems, UPS and smart metering. Dr. Savaghebi was a Guest Editor of Special Issue on Power Quality in Smart Grids, IEEE Transactions on Smart Grid and also a member of Task Force on Microgrid Stability Analysis and Modeling, IEEE Power and Energy Society. He is an Associate Editor of IEEE Access, a member of Technical Committee of Renewable Energy Systems, IEEE Industrial Electronics Society as well as Vice-Chair of sub-committee on Smart Buildings, IEEE Power and Energy Society.

Josep M. Guerrero (S'01-M'04-SM'08-FM'15) received the B.S. degree in telecommunications engineering, the M.S. degree in electronics engineering, and the Ph.D. degree in power electronics from the Technical University of Catalonia, Barcelona, in 1997, 2000 and 2003, respectively. Since 2011, he has been a Full Professor with the Department of Energy Technology, Aalborg University, Denmark, where he is responsible for the Microgrid Research Program (www.microgrids.et.aau.dk). From 2014 he is chair Professor in Shandong University; from 2015 he is a distinguished guest Professor in Hunan University; and from 2016 he is a visiting professor fellow at Aston University, UK, and a guest Professor at the Nanjing University of Posts and Telecommunications.
His research interests is oriented to different microgrid aspects, including power electronics, distributed energy-storage systems, hierarchical and cooperative control, energy management systems, smart metering and the internet of things for AC/DC microgrid clusters and islanded minigrids; recently specially focused on maritime microgrids for electrical ships, vessels, ferries and seaports. Prof. Guerrero is an Associate Editor for a number of IEEE TRANSACTIONS. He has published more than 450 journal papers in the fields of microgrids and renewable energy systems, which are cited more than 30,000 times. He received the best paper award of the IEEE Transactions on Energy Conversion for the period 2014-2015, and the best paper prize of IEEE-PES in 2015. As well, he received the best paper award of the Journal of Power Electronics in 2016. During five consecutive years, from 2014 to 2018, he was awarded by Thomson Reuters as Highly Cited Researcher. In 2015 he was elevated as IEEE Fellow for his contributions on "distributed power systems and microgrids."